Received: 3 November 2021 | Revised: 26 January 2022 | Accepted: 29 January 2022

DOI: 10.1002/jmor.21459

RESEARCH ARTICLE

JOURNAL OF morphology WILEY

Neurotransmission and neuromodulation systems in the learning and memory network of *Octopus vulgaris*

Naama Stern-Mentch[1] | Gabrielle Winters Bostwick[2,3] | Michael Belenky[1] | Leonid Moroz[2] | Binyamin Hochner[1]

[1]Department of Neurobiology, Silberman Institute of Life Sciences, Hebrew University, Jerusalem, Israel

[2]Department of Neuroscience and McKnight Brain Institute, and Whitney Laboratory for Marine Bioscience, University of Florida, Gainesville, Florida, USA

[3]Ocean Genome Atlas Project, San Francisco, USA

Correspondence
Binyamin Hochner, Department of Neurobiology, Silberman Institute of Life Sciences, Hebrew University, Jerusalem, Israel.
Email: benny.hochner@mail.huji.ac.il

Funding information
Human Frontiers Science Program, Grant/Award Number: RGP0060/2017; Israel Sciences Foundation (ISF), Grant/Award Numbers: 1425-2011, 1928-2015; National Science Foundation, Grant/Award Number: 1146575 1557923 1548121 1645219; United States - Israel Binational Science Foundation (BSF), Grant/Award Numbers: 2007-407, 2011-466; National Institute of Neurological Disorders and Stroke of the National Institutes of Health, Grant/Award Number: R01NS114491

Abstract

The vertical lobe (VL) in the octopus brain plays an essential role in its sophisticated learning and memory. Early anatomical studies suggested that the VL is organized in a "fan-out fan-in" connectivity matrix comprising only three morphologically identified neuron types; input axons from the median superior frontal lobe (MSFL) innervating *en passant* millions of small amacrine interneurons (AMs), which converge sharply onto large VL output neurons (LNs). Recent physiological studies confirmed the feedforward excitatory connectivity; a glutamatergic synapse at the first MSFL-to-AM synaptic layer and a cholinergic AM-to-LNs synapse. MSFL-to-AMs synapses show a robust hippocampal-like activity-dependent long-term potentiation (LTP) of transmitter release. 5-HT, octopamine, dopamine and nitric oxide modulate short- and long-term VL synaptic plasticity. Here, we present a comprehensive histolabeling study to better characterize the neural elements in the VL. We generally confirmed glutamatergic MSFLs and cholinergic AMs. Intense labeling for NOS activity in the AMs neurites were in-line with the NO-dependent presynaptic LTP mechanism at the MSFL-to-AM synapse. New discoveries here reveal more heterogeneity of the VL neurons than previously thought. GABAergic AMs suggest a subpopulation of inhibitory interneurons in the first input layer. Clear γ-amino butyric acid labeling in the cell bodies of LNs supported an inhibitory VL output, yet the LNs co-expressed FMRFamide-like neuropeptides, suggesting an additional neuromodulatory role of the VL output. Furthermore, a group of LNs was glutamatergic. A new cluster of cells organized as a "deep nucleus" showed rich catecholaminergic labeling and may play a role in intrinsic neuromodulation. In-situ hybridization and immunolabeling allowed characterization and localization of a rich array of neuropeptides and neuromodulators, likely involved in reward/punishment signals. This analysis of the fast transmission system, together with the newly found cellular elements, help integrate behavioral, physiological, pharmacological and connectome findings into a more comprehensive understanding of an efficient learning and memory network.

KEYWORDS
acetylcholine, catecholamine, cephalopods, dopamine, evolution, GABA, glutamate, LTP, mollusks, neuromodulators, neuronal circuits, neuropeptides, neurotransmitters, nitric oxide, serotonin, synapse

1 | INTRODUCTION

Cephalopods are critical reference species in neuroscience, with multiple examples of genomic and neuronal innovations and convergent evolution (Albertin et al., 2012; Striedter et al., 2014; Yoshida et al., 2015; Nesher et al., 2020; Turchetti-Maia et al., 2017; Albertin et al., 2015: Liscovitch-Brauer et al., 2017). Octopuses are known for their highly flexible behavior, which relies on various forms of associative learning, including observational learning (Alves et al., 2008; Amodio & Fiorito, 2013; Boal, 1996; Boycott, 1954; Fiorito & Scotto, 1992; Hanlon & Messenger, 2018; Mackintosh, 1965; Maldonado, 1963; Maldonado, 1965; Moriyama & Gunji, 1997; Papini & Bitterman, 1991; Sutherland, 1959; Wells, 1978). Their behavioral flexibility also includes solving the problems of complex motor tasks through learning strategy (Fiorito et al., 1990; Gutnick et al., 2011; Gutnick et al., 2020; Richter et al., 2015; Richter et al., 2016 see review Nesher et al., 2020) Behavioral lesion and stimulation studies have implicated the vertical lobe (VL, Figure 1) as a major part of the octopus learning system (Boycott, 1961; Boycott & Young, 1958; Fiorito & Chichery, 1995; Graindorge et al., 2006; Shomrat et al., 2008). In addition, the anatomical organization of the VL resembles other well-studied brain structures involved in learning and memory, like the insect mushroom-body and the mammalian hippocampus (Young, 1995). The development of the VL slice preparation allowed physiological investigation of the VL (Hochner et al., 2003; Hochner et al., 2006), revealing a robust activity-dependent long-term potentiation (LTP), whose expression is similar to that in the hippocampus. This LTP is important for acquiring long-term memory, as saturation of the LTP mechanism by electrical stimulation prior to training in a passive avoidance task, impaired the transition of short- into long-term memory (Shomrat et al., 2008).

1.1 | The MSFL-VL memory system

The median superior frontal lobe (MSFL), a brain region thought to integrate sensory information (Figure 1), appears to contain only one morphological type of neuron. Their axonal projections form the distinct MSFL tract into the VL neuropil (Young, 1971). The tract runs in an outer neuropil layer between the deep neuropil and the external cell bodies creating the cortices of the five VL lobuli (Figure 1c,d). The VL cortices contain two main classes of cell bodies, a majority of small amacrine cells (AMs; ~3–6 μm dia.), whose neurites run radially into the center of the VL medulla, and a relatively small number of large neurons (LNs; ~10–17 μm dia.) lying in the inner zones of the cortex, either singly or in clusters of up to six (Figure 1c,d). Both AMs and LNs are morphologically typical invertebrate monopolar neurons (Bullock & Horridge, 1965; Young, 1971).

The afferent axonal bundles from the MSFL are distributed throughout the whole VL (Young, 1971), with each MSFL axon making *en passant* synapses with a yet unknown number of AM interneurons along its length (Figure 1c,d). A second input to the VL is less defined but may carry pain (punishment) and reward signals. These axons enter the VL from the subVL (Figure 1b) and ramify in the VL neuropil (Gray, 1970). The LN trunks run radially into the medulla, where they give off dendritic collaterals, which branch profusely in the more central regions of the neuropil. Their axons project to the subvertical lobe (subVL), but little is known about other possible targets.

The general connectivity of the VL can be described as a feedforward fan-out fan-in, bi-synaptic network (Shomrat et al., 2011), whose suggested connectivity is shown in Figure 1c,d (Gray, 1970; Young, 1971, 1995). The 1.8 million MSFL neurons diverge ("fan out") to innervate 25 million AM interneurons (Figure 1c,d; Gray, 1970; Young, 1971). The fan-in connection of the AMs onto merely 65,000 efferent LNs is mediated by serial synapses, in which the AM neurites are postsynaptic to the MSFL axon terminals and presynaptic to the spines of the LN dendrites (Figure 1d; Gray, 1970). The LNs are presumed to be the only output of the VL (Young, 1971), their axons leave the VL ventrally in organized bundles or roots.

The VL bi-synaptic fan-out fan-in network, like the presumed association neural networks of the mammalian hippocampus and the insect mushroom bodies (Heisenberg, 2003; Wolff & Strausfeld, 2016; Young, 1991, 1995), is arranged similarly to feedforward two-layered artificial "perceptron" networks (Rosenblatt, 1958). Provided that one of the two synaptic layers is endowed with long-term synaptic plasticity, these produce computational functions such as association and classification (Shomrat et al., 2011; Vapnik, 1998).

The MSFL-VL system is important for visual learning, while the median inferior frontal lobe (MIFL) and subfrontal lobe (subFL) form the main part of the touch learning system (Wells, 1978). The morphological organization of the MIFL-subFL system resembles that of the MSFL-VL complex, but it is significantly smaller (Figure 1a,b; Young, 1971, 1991).

Different ultrastructure of the synaptic vesicles in this system (Young, 1971) indicates the recruitment of different neurotransmitters. Pharmacological experiments were performed to elucidate putative neurotransmitters and neuromodulators of the VL system (Figure 1c,d; for review (Turchetti-Maia et al., 2017). The fan-out input to the AMs appears to be glutamatergic, while the fan-in input to the LNs is cholinergic (Shomrat et al., 2011), with no direct connections from the MSFL neurons to the LNs. Hochner et al. (2003) found no indication that the LTP induction mechanism in the *Octopus* VL is NMDA-mediated. This is not surprising since the pharmacology of

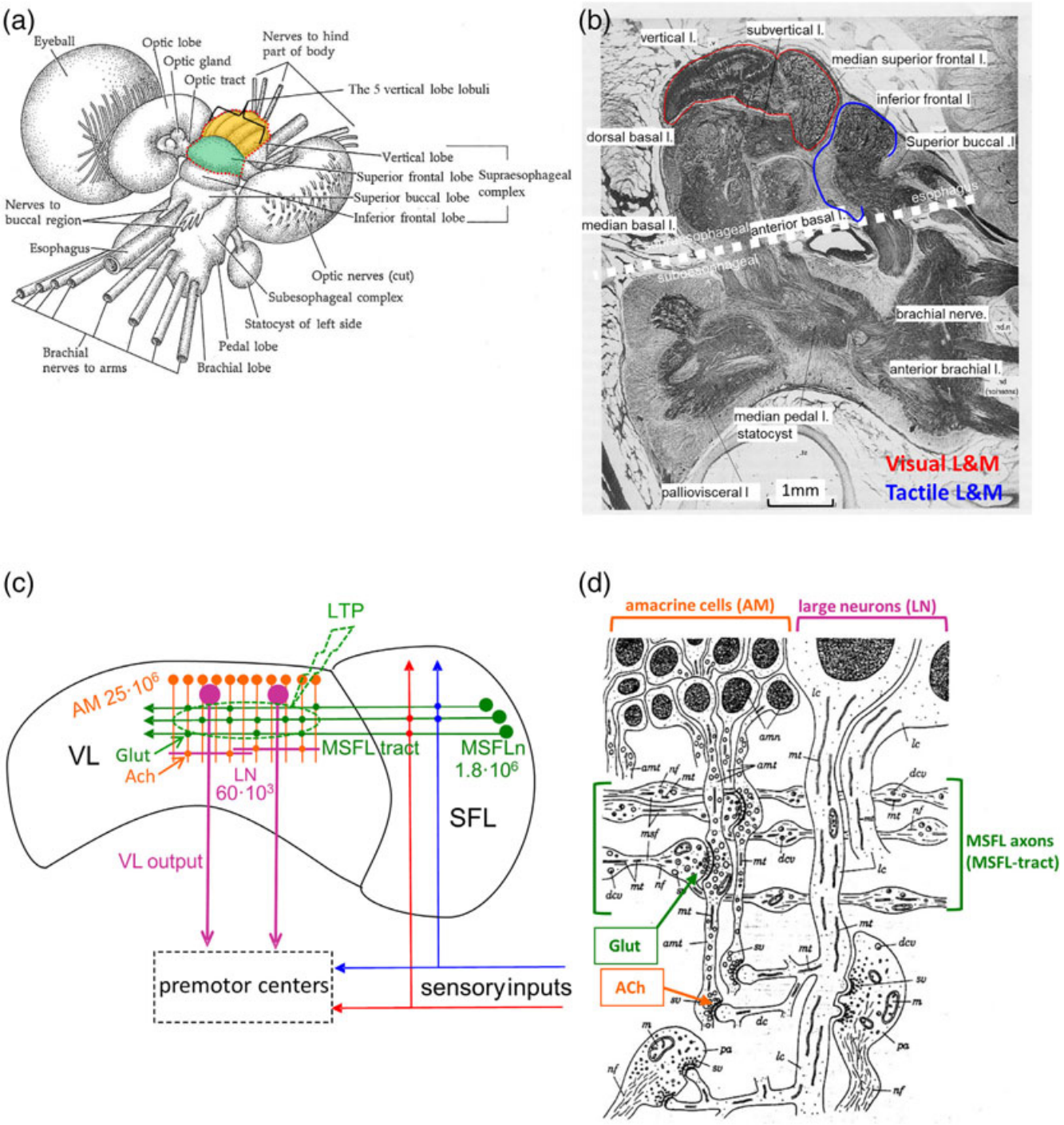

FIGURE 1 The morphological organization of the octopus brain (a) the centralized brain of *Octopus vulgaris* in anterior-dorsal view. The supraesophageal brain complex includes the superior frontal lobes (SFL, green) and the vertical lobe (VL, orange), which consists of five cylindrical gyri. Red dotted line outlines the area of the visual learning system at the most dorsal part of the supraesophageal complex. The inferior frontal lobe (IFL), part of the touch learning system, lies ventrally and slightly anterior to the SFL (modified from Brusca & Brusca, 1990). (b) Sagittal section of the sub and supraesophageal brain complexes showing the dorsally located median SFL (MSFL)-VL system (red line), the median IFL (MIFL)-subFL system (blue line), and the organization of the other lobes (modified from Nixon & Young, 2003). (c) A schematic wiring diagram of the neural elements of the VL system, showing the basic connectivity, types, and numbers of cells in the MSFL-VL system. Neurotransmitters and synaptic areas where long-term potentiation (LTP) occurs are marked (after Shomrat et al., 2011). (d) A classic diagram summarizing the basic circuitry of the VL (adapted from Gray, 1970) with superimposed neurotransmitters as inferred from pharmacological studies (Shomrat et al., 2011). *amn*, amacrine interneurons; *amt*, amacrine trunk; *dc*, dendritic collaterals of large neurons; *dcv*, dense core vesicle; *co*, cortex of vertical lobe; *h*, hila of vertical lobe; *lc*, body or trunk of the large neurons; *m*, mitochondrion; *mt*, microtubule; *nf*, neurofilaments; *pa*, possible nociceptive axon input to the large neurons; *sv*, synaptic vesicles

NMDA receptors in mollusks often differs significantly from that in vertebrates (e.g., Moroz et al., 1993) and a number of ionotropic glutamate receptors have been described in cephalopods (Di Cosmo et al., 2006; Di Cosmo et al., 1999; Di Cosmo et al., 2004; Moroz et al., 2021). This likely NMDA-independent LTP involves an exclusively presynaptic mechanism resembling the presynaptic expression of the non-associative LTP of mossy fiber synaptic input to the CA3 pyramidal cells of the hippocampus (Kandel et al., 2012; Yeckel et al., 1999). Yet, the LTP in the *Octopus vulgaris* VL appears to be mediated by a novel mechanism, whereby an activity-dependent constitutive elevation in nitric oxide (NO) mediates the LTP expression through NO-mediated presynaptic facilitation of transmitter release from the MSFL axon terminals (Turchetti-Maia et al., 2018).

Various neuromodulators appear to be active in the *Octopus* VL. 5-HT causes presynaptic facilitation of the glutamatergic MSF-AM synapses (Shomrat et al., 2010), possibly also indirectly enhancing the activity-dependent induction of LTP (Shomrat et al., 2010). Octopamine (OA), an excitatory neuromodulator in mollusks (Vehovszky et al., 2004; Wentzell et al., 2009) provokes a short-term facilitatory effect in the VL, like 5-HT. However, unlike 5-HT, OA attenuates LTP induction. Therefore, it was proposed that 5-HT and OA transmit punishment and reward signals into the VL where they enhance or suppress, respectively, the associative strengthening of synaptic connections (see Turchetti-Maia et al., 2017).

Although specific neurotransmitters and neuromodulators have been found in the octopus brain (Messenger, 1996; Shomrat et al., 2010; Shomrat et al., 2011; Taghert and Nitabach 2012; Tansey, 1979; Winters et al., 2020; Shigeno & Ragsdale, 2015), little is known about their precise distribution in the MSFL-VL learning and memory system. Here, we characterize the anatomical distribution of candidates for neurotransmitter and neuromodulation systems in the MSFL-VL with special attention to those identified in the physiological analysis of VL connectivity, plasticity and neuromodulation (see Shomrat et al., 2015; Turchetti-Maia et al., 2017). Our anatomical findings advance the understanding of the functional organization of the "fan-out fan in" network. We show here that this network is more complex than the previously reported two simple homogenous neuron layers. Lastly, we characterize the distribution of possible neuromodulators and identify and generally localize candidate neuropeptides involved in learning.

2 | MATERIALS AND METHODS

Adult *Octopus vulgaris* Cuvier, 1797 weighing ~150–450 g were captured off the Mediterranean coast of Israel. They were kept individually in closed synthetic seawater aquaria (80–100 L) with biological and chemical filters and maintained at 18°C on a 12 h light/dark cycle (Hebrew University) or in semi-open seawater systems, both light- and temperature-controlled (Ruppin Faculty of Marine Sciences, Michmoret, Israel). Animals were acclimatized to the laboratory for at least 2 weeks before experiments, conforming to the ethical principles of EU Directive 2010/63/EU, the principle of the 3Rs (Replacement, Reduction and Refinement), and minimization of suffering (see Fiorito et al., 2014, 2015).

Animals were deeply anesthetized in fresh seawater supplemented with 2% ethanol and 55 mM $MgCl_2$ (Shomrat et al., 2008). The brain was removed through a dorsal opening of the cartilaginous brain capsule. For most histochemical procedures, the brain was immediately fixed by immersion 4 h-overnight in 4% PFA in artificial seawater (ASW; Shomrat et al., 2008) or 0.1 mol l^{-1} phosphate-buffered saline (PBS), pH 7.4 at 4°C. Table 1 gives the fixation and preservation solutions used for each primary antibody. Brain slices were obtained as described in Shomrat et al. (2008). After washing with ASW or PBS, the fixed supraesophageal mass was glued with acrylic glue to a vibratome stage (Leica, VT1000 S). 50–90 μm sagittal, transverse or horizontal sections were used for immunohistochemistry (IHC; Shomrat et al., 2010).

For cChAT confocal microscopy experiments, after fixation and washing, tissues were immersed for at least 24 h in PBS containing 30% sucrose at 4°C, frozen on the microtome base with dry ice, and sectioned sagittally on a sliding microtome (40 μm). Free-floating sections were collected in ice-cold PBS. Each type of marker was tested on a minimum of two brains, eight slices per brain.

2.1 | Immunohistochemistry

An immunoperoxidase procedure was performed on free-floating sections for the immunohistochemical detection of target epitopes in electron microscopy (EM) and light microscopy (LM) sections, similar to the protocol in Shomrat, Feinstein, Klein, & Hochner, 2010; differences are noted in Table 1).

2.1.1 | Immunoperoxidase labeling

After slices were incubated in primary antibody (Table 1) and washed, they were incubated for 3 h, at room temperature (RT) in biotinylated secondary antibody (1:600 goat anti-rabbit, Vector Laboratories, USA). The sections were placed in avidin-biotin peroxidase complex (ABC Elite, Vector Laboratories, USA) for 1 h at RT. PBS was used after each step. Peroxidase activity was visualized as a brown precipitate by reacting the sections for 3–7 min at RT with a solution containing 0.04% 3-3diaminobenzidine-tetrachloride (DAB) and 0.006% H_2O_2. When picric acid was used for pre-staining tissue preservation, the DAB solution also included 0.4% nickel ammonium sulfate in 50 mM Tris–HCl buffer (pH 7.6) to yield a dark blue precipitate. The reaction was stopped by rinsing with PBS or Tris–HCl buffer, accordingly. For EM, the reaction product was intensified and substituted with silver/gold particles, as described by (Livneh et al., 2009). For control experiments, sections were processed as described above but without the primary antibody, resulting in no specific staining.

Sections for light microscopy were mounted on SuperFrost Plus slides (Menzel Glaser, Germany) and air-dried. The sections were then dehydrated in a graded ethanol series (70%–100%), cleared with

TABLE 1 Antibodies, concentrations, information on methods, fixation, sample processing and provider

Antibodies	Host species	Dilution for LM	Dilution for confocal	Dilution for EM	Method	Fixatives and processing	Provider
Anti-glutamate (p)	Rabbit	1:5000–1:15,000			ABC	4% PFA; VT	ImmunoSolutions (IG1006)
Anti-choline-acetyltransferase of the common type (cChAT) (p) (Sakaue et al. 2014)	Rabbit	1:5000–1:10,000	1:500	1:2500–1:5000	ABC; EM; FLUO	4% PFA and 0.2% PA; VT or MCT	Prof. H. Kimura, and Dr., Jean-Pierre Bellier Molecular Neuroscience Research Center,Shiga University of Medical Science,Japan
Anti GABA (p)	Rabbit	1:10,000		1:5000–1:10,000	ABC; EM	4% PFA and 0.25% GA; VT	Prof. Misha Belenky and Prof. Péter Somogyi, Oxford University, Oxford, UK
Anti-Tyrosine Hydroxylase (TH) (p)	Sheep	1:500			ABC	4% PFA and 0.2% PA or 4% PFA and 0.25% GA; VT	Prof. Misha Belenky

Note: *p* polyclonal *ABC* avidin-biotin complex, *GA* glutaraldehyde, *PFA* paraformaldehyde, *PA* picric acid, *EM* electron microscope, *FLUO* immunofluorescence method, *VT* vibratome, *MCT* microtome.

xylene, and cover-slipped with Enthellan for observation under an Olympus BX43 microscope.

2.1.2 | Immunofluorescence

Slices were incubated in rabbit anti-cChAT primary antibody (Table 1) and washed (omitting incubation in H_2O_2). Samples were then incubated for 2 h with anti-rabbit Alexa Fluor 594 secondary antibody (1:500; Thermo Fisher Scientific). Slices were washed and mounted on microscope slides. Fluorescent counterstaining of cell nuclei was carried out in a PBS solution with 0.1 μg/ml 4′,6-diamidino-2-phenylindole (DAPI; Roche Molecular Biochemicals, Indianapolis, IN, USA). Fluorescence was detected, analyzed and photographed with an Olympus BX43 microscope or with an Olympus FV-1200 confocal microscope. Alexa Fluor 594 was excited with the 561 nm laser and the emission wavelength was 570–620 nm. Images were prepared using NIH ImageJ software (Bethesda, MD, USA).

For electron microscopy, the sections were post-fixed, treated and observed according to Shomrat et al. (2010). Photomicrographs were unaltered except for brightness/contrast enhancement.

2.1.3 | NADPH-diaphorase staining

The brain tissue was fixed by immersion in 4% PFA in ASW pH 7.4 at 4°C overnight. In later experiments, 0.25% glutaldehyde (GA) was added to the fixation solution. After slicing (50–100 μm), sections were analyzed for NADPH-diaphorase activity according to (Hope & Vincent, 1989) and modifications by Moroz (Moroz, 2000; Moroz et al., 2000). At the final stages, slices were dehydrated in ethanol, cleared in xylene, mounted on SuperFrost Plus slides (Menzel Glaser, Germany) and viewed with Olympus SZX16 stereo and Olympus BX43 microscopes. Specificity of NADPH-diaphorase staining was tested in control experiments in which tissue sections were incubated in the reaction solution as described, except that β-NADPH or NBT were omitted. All chemicals for this procedure were purchased from Sigma–Aldrich unless otherwise indicated

2.2 | In situ hybridization

All procedures were carried out at room temperature unless otherwise stated. Samples were agitated only during antibody incubation and washes. Particular attention was paid to maintaining an RNase-free environment. To help avoid contamination, solutions prepared according to Jezzini et al. (2005) were made in small batches in disposable sterile 50 ml plastic centrifuge tubes (Corning Incorporated, NY, USA; Cat. No. 430921). The specimens were incubated in disposable sterile 24-well cell culture plates (Corning Incorporated, NY, USA; Cat. No. 3524).

2.2.1 | In situ hybridization probe preparation

The molecular information for target mRNAs and sequences is summarized in Data S1. Digoxigenin-labeled antisense RNA probes were transcribed in vitro using SP6 or T7 polymerases (according to the insert's specific orientation into the plasmid) from full-length cDNA clones, ligated into p-GEM T vector (Promega) and linearized with the

appropriate restriction endonucleases. Full-length sense probes were used for negative controls. One μl of the restriction digest ran on a 1% agarose gel with ethidium bromide staining to check for quality of the reaction, and the remainder was purified using a PCR purification kit (Qiagen). Typically, 13 μl of the purified linearized plasmid (approx. 1 μg plasmid) was used as a template in the probe synthesis reaction. This was carried out using the DIG RNA Labeling Kit (SP6/T7; Roche; Cat. No. 1175025) according to the manufacturer's instructions (13 μl template, 2 μl NTP labeling mix, 2 μl 10× transcription buffer, 1 μl RNase inhibitor, 2 μl SP6 or T7 RNA polymerase, 37°C for 2 h). The reactions were stopped by adding 2 μl 0.2 mol l^{-1} EDTA, pH 8.0. The NTP labeling mix contained either DIG-11-UTPs (DIG RNA Labeling Mix, Roche; Cat. No. 1277073) for synthesis of DIG-labeled probes or Fluorescein RNA Labeling Mix (Roche; Cat. No. 1685619) for synthesis of fluorescein-labeled probes. The quality of plasmids, restriction digests, and synthesized probes was checked on a 1% agarose gel with ethidium bromide staining prior to use. Probes up to 1 kb or longer were used at full length (see CNS preparation and details in Supporting Information).

2.2.2 | CNS processing and probe hybridization

In situ hybridization (ISH) experiments were performed as described previously (Jezzini et al., 2005; Winters et al., 2020; Moroz & Kohn, 2010) with minor modifications. Immediately following removal from anesthetized animals, the supraesophageal mass was fixed in 4% formaldehyde in PBS, pH 7.4 overnight at 4°C. The brain mass was then washed in three 15 min changes of PBS before being placed in a tub with fresh PBS and sectioned at 300–450 μm. All slices were washed three times with PBS, transferred to PTW (0.1% Tween 20 in PBS) for 10 min and subsequently dehydrated in sequential 10 min incubations in methanol (30%–70%) in PTW, followed by 100% methanol at −80°C overnight. The slices were then shipped from the Hebrew University to the University of Florida, St. Augustine, on dry ice. They were rehydrated by sequential 10 min incubations in methanol (70%–30%) in PTW followed by 100% PTW for 15 min. They were then washed with 0.3% Triton X-100 in PBS for 10 min, PBS for 10 min, and PTW for 5 min. Proteinase K (Roche Diagnostics) was added to the PTW to a final concentration of 10 μg Proteinase K per 1 ml PTW (typically around 0.6 μl Proteinase K per 1 ml PTW). The slices were incubated at RT for 20 min (or until they started to appear slightly translucent around the edges). Proteinase K activity was terminated by transferring slices to 4% formaldehyde in PBS for 20 min at 4°C. Following post-fixation in 4% formaldehyde, the slices were washed in two changes of PTW followed by two changes of PTW and three changes of TEA HCl (0.1 mol l^{-1} triethanolamine hydrochloride adjusted to pH 8.0 with NaOH). With the slices in a 1 ml volume of 0.1 mol l^{-1} triethanolamine hydrochloride adjusted to pH 8.0 using sodium hydroxide, 2.5 μl of acetic anhydride was added slowly to the TEA HCL while stirring. The slices were left for 5 min before adding an additional 2.5 μl acetic anhydride while stirring, followed by another 5 min incubation. Next, the slices were washed in three changes of PTW before being transferred to hybridization buffer (HB: 50% formamide, 5 mM EDTA, 5× SSC (20× SSC: 3 mol l^{-1} NaCl, 0.3 mol l^{-1} sodium citrate, pH 7.0), 1× Denhardt solution (0.02% ficoll, 0.02% polyvinylpyrrolidone, 0.02% bovine serum albumin), 0.1% Tween 20, 0.5 mg/ml yeast tRNA (GIBCO BRL)). The slices were then left overnight in HB at −20°C before prehybridization incubation for 6–8 h at 50°C the next day. Next, 2–6 μl (~1 μg/ml) of each probe was added and hybridization allowed to proceed for 12–14 h at 50°C.

2.2.3 | Immunological detection

Immunological detection was performed using antidigoxygenin-AP Fab antibody fragments at a dilution of 1:2000 (Roche Diagnostics, Mannheim, Germany). After probe hybridization, the slices were washed in 50% formamide/5× SSC/1% SDS (sodium dodecyl sulfate, Fisher 20% solution BP1311) for 30 min, then 50% formamide/2× SSC/1% SDS for 30 min at 60°C, and two 30 min changes of 0.2× SSC at 55°C. Slices were transferred to PBT (0.1% Triton-X 100, 2 mg/ml bovine serum albumin, in PBS; pH 7.4) for 20 min followed by two 20 min changes of PBT at RT. Goat serum was added after the third change to a concentration of 10% by volume, and the slices were then incubated for 90 min at 4°C with gentle shaking, after which the sections were placed in 1% goat serum in PBT. Alkaline phosphatase-conjugated antibodies were then added and incubation proceeded for 12–14 h at 4°C with gentle shaking

2.2.4 | Development using the NBT/BCIP alkaline phosphatase substrate: Single probe labeling

After incubation with antibody, the slices were transferred to PBT at 4°C and washed in three 30 min changes of PBT at 4°C followed by three 5 min changes of filtered NBT/BCIP detection buffer (NDB: 100 mmol l^{-1} NaCl, 50 mmol l^{-1} $MgCl_2$, 0.1% Tween 20, 1 mmol l^{-1} levamisol, 100 mmol l^{-1} Tris–HCl; pH 9.5) at 4° C. 20 μl/ml of NBT/BCIP stock solution (NBT/BCIP: 18.75 mg/ml nitro blue tetrazolium chloride, 9.4 mg/ml 5-bromo-4-chloro-3-indolyl phosphate toluidine salt in 67% dimethyl sulfoxide, Roche; Cat. No. 1681451) was added to the third change of NDB while stirring thoroughly until completely dissolved. The slices were kept on ice in the dark, and every 10 min were monitored briefly for staining to avoid excessive exposure to light. Development was terminated after cell-specific labeling was clearly visible and before excessive background began to appear. Development was stopped by transferring the slices to 4% formaldehyde in methanol for 60 min at 4°C followed by a final transfer into 100% ethanol at 4°C, immediately followed by washing in two 10 min changes of 100% ethanol at 4°C. The slices were cleared in methylsalicylate (for about 1 min or until they sank to the bottom) and mounted on microscope slides in Permount (Fisher).

Images were acquired digitally with an Olympus DP-73 camera mounted on Olympus SZX16 stereo and Olympus BX43 binocular microscopes. The diameters of immunoreactive cells were measured on photomicrographs of sagittal and transverse sections with LITE (Leica) or FIJI (ImageJ) software.

3 | RESULTS

3.1 | Canonical "fast" transmitters

3.1.1 | Glutamate

In situ hybridization (ISH) revealed that most of the cell bodies in the MSFL cortex and cortices of several other lobes expressed vesicular glutamate transporter VGLUT-encoding transcripts (Figure 2a). In contrast, the VL cortex was barely labeled. Light traces of VGLUT transcript expression appeared in the MSFL axonal projections in the outer ventral neuropil (Figure 2b, lower bracket), suggesting that respective mRNAs could be transported to distant neurites as in *Aplysia* (Puthanveettil et al., 2013).

Figure 3a shows similar results with IHC labeling for L-Glut; the cell bodies in the MSFL cortex showed stronger glutamate immunoreactivity (L-glu-IR) than the generally pale L-Glut labeling in the neighboring AM cell bodies of the VL cortex. Thus, some MSFL neurons are indeed potential sources for glutamatergic input to the VL (Hochner et al., 2003; Shomrat et al., 2011). In addition, L-Glut antibody revealed clusters of L-Glut-IR LN (18–30 μm dia.) with positively labeled neurites detected in several individual cells. This group of cells was organized separately from the cell body cortex as a "deep nucleus" located at the MSFL-VL border and likely interacts with the main MSFL-VL circuitry (Figure 4).

The VL showed intense granular L-Glut-IR in the area of the MSFL axonal projections (Figure 3b,c). This particularly dark labeling at the lower region of the outer neuropil was localized at the area of the *en passant* synaptic connections right at the junction of the AM trunk and the MSFL tract (Gray, 1970; Shomrat et al., 2011), probably marking the synaptic varicosities rich in glutamatergic vesicles.

L-Glu IR was also found in medium to large LN cells (6–12.5 μm dia.) in the inner half of the VL cell cortex (Figure 3a–d), either lying alone or as a small group among unstained cell bodies. Remarkably, these positively stained cells were located in the dorsal cell layer in classic locations of the LNs. Indeed, large VGLUT transcript-expressing cell bodies were revealed in similar cortical areas (Figure 2b). Thus, some of the LNs in the VL appear to be glutamatergic.

The L-Glu-IR LNs in the ventral cell cortex appeared more dense and visible neuronal processes projected mainly inward toward the cell layers and not into the neuropil (Figure 3c,d,d2, arrowheads). These ventral glutamate-IR processes hint that some neurites do not necessarily exit with the common LN roots crossing the VL hila, (Gray, 1970) instead, may maneuver their way out of the VL through the small-cell body layer to the subVL ventral to the VL. These ventral LNs may thus represent a separate population or sub-type of LNs.

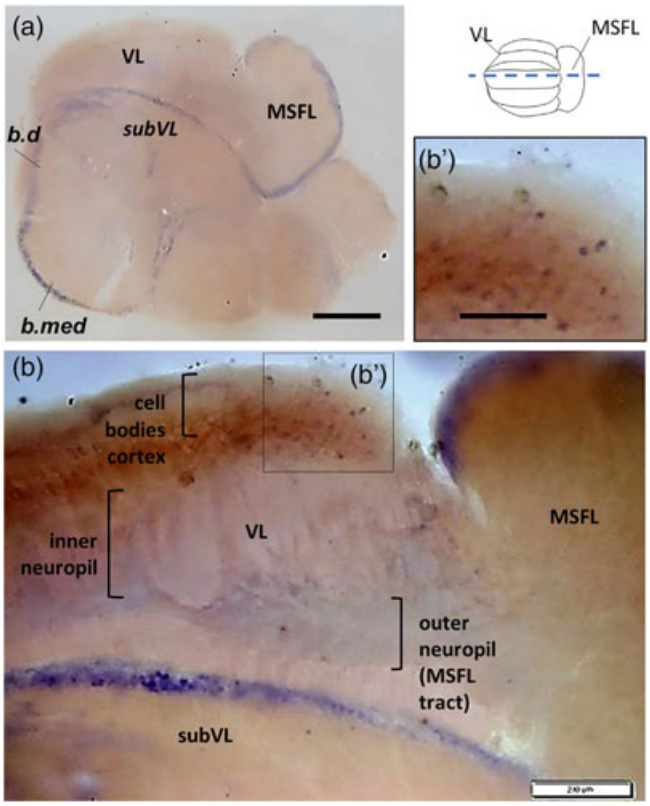

FIGURE 2 *Octopus vulgaris*, glutamate-transporter mRNA expression highlights the MSFL cell body cortex. Inset, schematic dorsal view of the *Octopus* MSFL-VL lobes. Dashed blue line represents the plane of sections in figure b (and all figures thereafter). (a) In situ hybridization (ISH) on a sagittal slice reveals expression of vesicular glutamate transporter (VGLUT) mRNA in MSFL cell cortex that contrasts greatly with the generally unlabeled cells of the VL cortex. Expression of VGLUT can also be seen in the cell layers of the subVL, basal dorsal (b.d), and basal medial (b.med) lobes. (b) Photomicrograph of in situ hybridized sagittal section showing VGLUT mRNA expressions in the ventral outer VL neuropil (MSFL-tract, lower bracket) in large cells in anterior regions (marked region). (b') magnification of VGLUT expressing cells of the dashed square region marked in b. Scale bar: 500 μm (a), 200 μm (b), 100 μm (b')

3.1.2 | Cholinergic system

We used cChAT antibody to identify cholinergic neurons (see Casini et al., 2012; D'Este et al., 2008; Sakaue et al., 2014). The semi-sagittal section in Figure 5 shows cChAT immunoreactivity in the MSFL-VL system compared with an unstained control section. While most positively labeled supraesophageal lobes did not exhibit a clear difference in labeling density between the neuropil and the cell body cortices, the VL is remarkable in the dense labeling of its inner neuropil, quite

distinct from the surrounding cell bodies. The global cChAT-IR of the MSFL was much weaker than the richly stained VL neuropil mass (Figure 5a).

Figure 6a,a' shows scattered fibers labeled in the MSFL neuropil with a slightly increased density in the outer neuropil below the cell body cortex. Similar results were obtained using fluorescent labeling

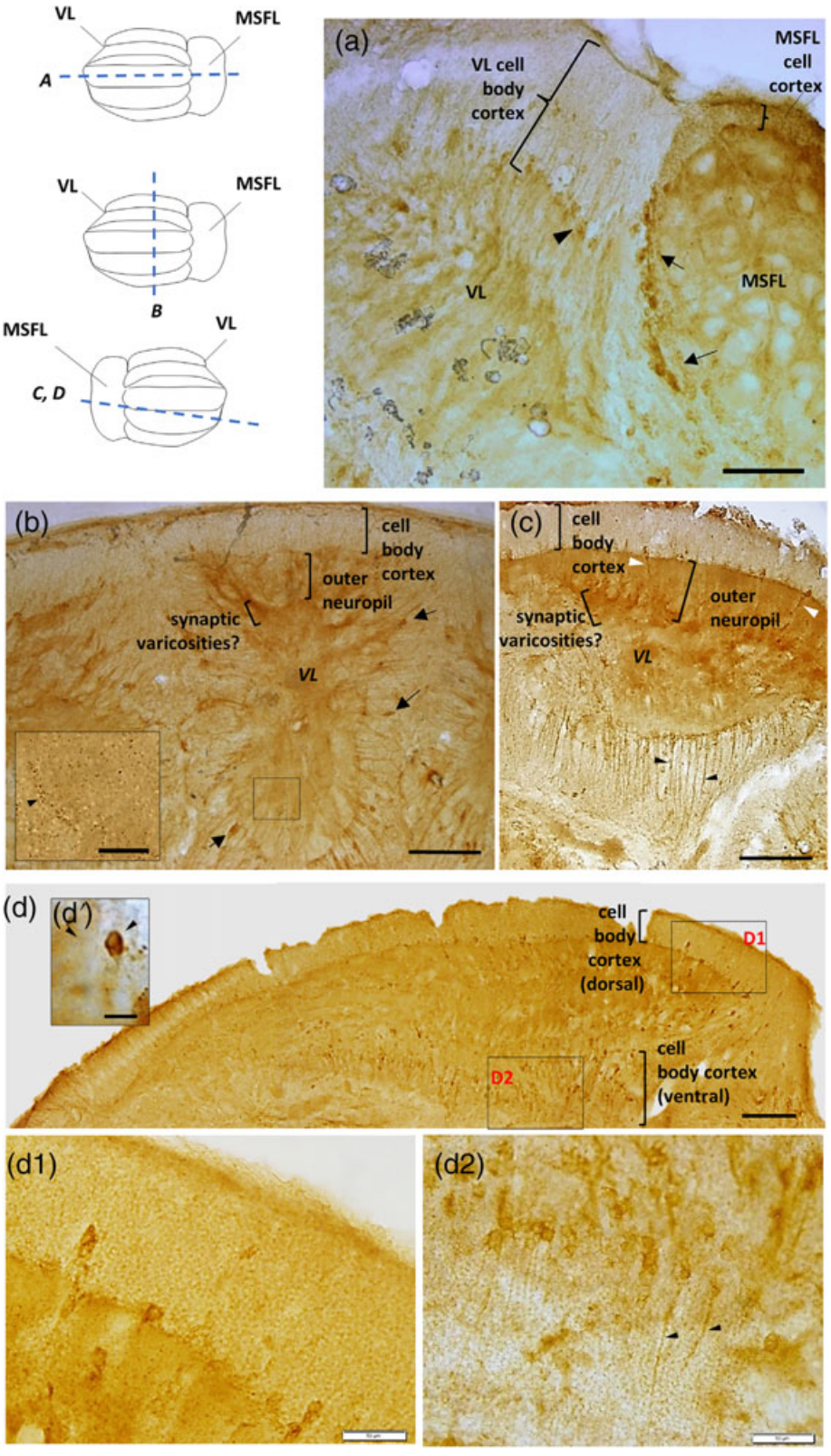

FIGURE 3 Legend on next page.

(Figure 6b). Thick cChAT-IR neuronal processes were visualized mainly in the posterior area of the outer MSFL neuropil. At the same time, scattered fibers were labeled in other parts of the MSFL neuropil, indicating cholinergic innervation of the MSFL outer neuropil.

The occasional cChAT granular markings detected along the MSFL tract axons in the outer neuropil are likely cChAT-IR AM trunks crossing through the unlabeled axons of the tract in the outer neuropil (Figure 7a,a',c,c', arrows). Fluorescence microscopy revealed dense labeling in the outer VL neuropil, again seemingly belonging to AM trunks running vertically over the unlabeled MSFL axon into the deep neuropil (Figure 7a). Associations of fluorescent labeling with presumed AMs trucks were seen by merging differential interference contrast (DIC) and fluorescent images captured with a confocal microscope (Figure 7a', arrow).

The intense cChAT-positive fiber labeling was similarly distributed in the neuropil across all five VL lobuli (Figure 7c). The cChAT-IR groups of bundled neurites running from the cell cortex crossed the unlabeled MSFL-tract fibers with gaps of ~25–30 μm between them and projected into the homogenous densely labeled inner neuropil. These results further support physiological findings, that at least some AMs are cholinergic (Shomrat et al., 2011).

cChAT-IR labeling was also observed along inter-lobulus connections running through the cell body cortex (Figure 7d,d'), suggesting cholinergic processes crossing between the VL lobuli. Note that Young (1971) considered the inter-vertical tracts crossing between the lobuli to be separate packets of MSFL tract fibers rather than AM projections. In addition, cChAT-IR labeling (Figure 7e) indicates that cholinergic fibers may run between the VL and the subVL through the VL hilum which connects the two lobes (Gray, 1970).

Electron microscopy showed a field in the inner medullary zone packed with extremities of transversely cut AM trunks with their characteristic clear agranular vesicles (Gray, 1970), which exhibited cChAT-IR (Figure 8a). Some of these amacrine processes showed synaptic connections with pale structures presumed to belong to the LN dendritic branches (Figure 8a; double membrane, arrowhead). In addition, strong cChAT-IR was revealed in neuronal structures and processes (Figure 8b). Some structures contained granulated vesicles varying in size up to 100 nm (Figure 8c). These vesicles did not appear to belong to the MSFL neurons, nor did they fit the classifications of amacrine vesicles or vesicles of "pain" fibers ascending into the lobules from below (Gray, 1970). Similar to the LM immunolabeling, visualization of the VL cell layers with EM barely revealed positive cChAT reactivity in the cytoplasm of the amacrine cell bodies (not shown).

Figure 9a displays a relatively similar cChAT reactivity pattern in the MIFL and the MSFL neuropil and rather intense darker brownish labeling of the VL and subFL neuropils (Figure 9a', lower bar). Cholinergic properties in the visual and tactile learning systems appear comparable. Yet, possibly because of the larger cell bodies of the subFL cortex (up to ~20 μm), cChAT-IR cell bodies were clearly visible in the outer cell layers of the subFL (Figure 9a', upper bar).

3.1.3 | γ-amino butyric acid

Figure 10a displays a general comparison between the γ-amino butyric acid (GABA) labeling in the MSFL, VL and the MIFL. GABA-IR processes were distributed mainly in the outer MSFL neuropil plexus. The intensely labeled processes appear to carry dark GABA-IR swellings, possibly synaptic varicosities (Figure 10a1'). The dense and widespread GABA-IR probably derives from the external inputs to the MSFL described by Young (1971), rather than local MSFL innervation, suggesting inhibitory input to the MSFL. In both the MSFL and MIFL, the dense punctuated GABA-IR seemed to encircle fascicles of neuropilar structures (Figure 10a1,a3).

Strong GABA-IR labeling was detected in a distinct group of LN cell bodies (~6–13 μm dia.) in the VL (Figure 11b, arrows) and their neuronal processes (Figure 11b'), which are remarkably organized along the dorsal and ventral inner margin of VL cell body cortex. These morphological characteristics fit the LN described byYoung and Gray, and therefore our findings confirm that this group of LN mediates the inhibitory output of the VL (Shomrat et al., 2008). An intriguing conspicuous coloration was observed in the dorsal portion of

FIGURE 3 *Octopus vulgaris*, distribution of glutamate-positive cell bodies and neuronal processes in the VL. (a) MSFL cell body cortex reveals stronger glutamate immunoreactivity (L-Glu-IR) than the global pale L-Glu labeling in the neighboring cell body cortex of the VL. L-Glu-IR also reveals a group of large cells at the border between the MSFL and VL (arrows). Arrowhead marks large cells positively labeled in the inner margin of the VL cell body cortex. (b) Photomicrograph of a transverse section of the VL showing L-Glu-IR in relatively large cells (6–13 μm dia.). Intensified markings are localized at the border area between the outer and inner neuropil, suggesting this area as a site of greater synaptic densities (lower bracket). Large cell bodies are labeled (arrows). (b') Magnifications of the area marked in b showing granular labeling in the VL neuropil. Intensified granular L-Glu labeling in the border zone between the outer and inner neuropil (circling the center of the medulla; arrowhead), again suggesting a unique compartmentalized area with high synaptic densities. (c) Light micrograph of the sagittal section showing darkened markings in the border area of the outer and inner neuropil similar to those seen in transverse section in b. L-Glu-IR large cell bodies are localized in the dorsal region, their processes projecting into the neuropil (white arrowheads), while glutamatergic processes from large cells in the ventral region mainly project inwards to the ventral cell body cortex or to the subVL (black arrowheads). (d) Photomicrograph of the sagittal section showing glut-IR of relatively large cells distributed in the inner layers of the dorsal and ventral cell cortices surrounding the VL lobuli. The L-Glu positively labeled cells in the dorsal cortical cell layer are organized in a typical row along the inner margin of the cell cortex, resembling the appearance and organization of the large neurons (LNs). The L-Glu-IR cells in the ventral region are more crowded and uniquely organized, differing from "typical" LNs (lower bracket). (d') Enlarged example of glutamate-IR cell (~9 μm; arrowhead, right) in the VL, taken from section similar to that in d, neighboring a cell similar in size but lacking glutamate-IR (arrowhead, left). (d1, d2) Magnification of L-Glu-IR large cells in the dorsal and ventral cortex layers seen in dashed squares marked in d. Scale bar: 200 μm (a–d), 50 μm (b', d1, d2), 10 μm (d')

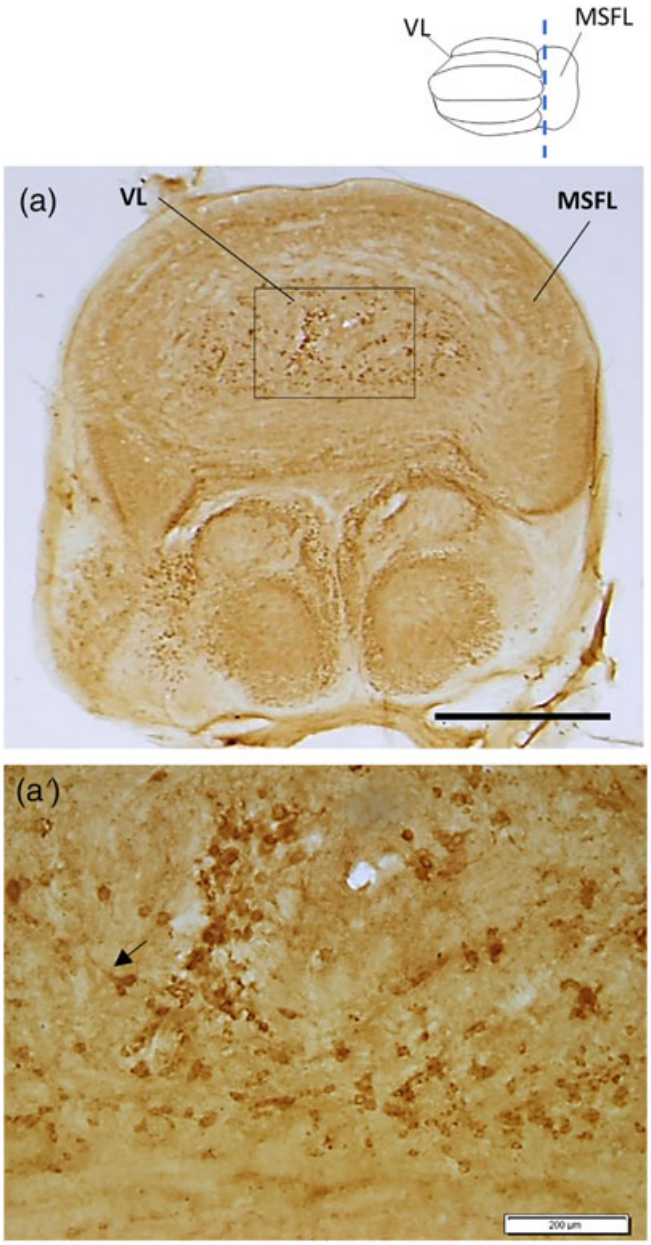

FIGURE 4 *Octopus vulgaris*, glutamate immunohistochemistry reveals a "deep nucleus" in the VL-MSFL system. (a) The transverse section shows the L-Glu positive large cell bodies (18–30 µm in diameter) in the area between the MSFL and VL. They are distinctly organized as a "deep nucleus." (a') Higher magnification of the area marked in (a) showing large L-Glu-IR cell bodies. Positive neuronal processes projecting from these cells can also be seen (arrow). Scale bar: 1 mm (a), 200 µm (a')

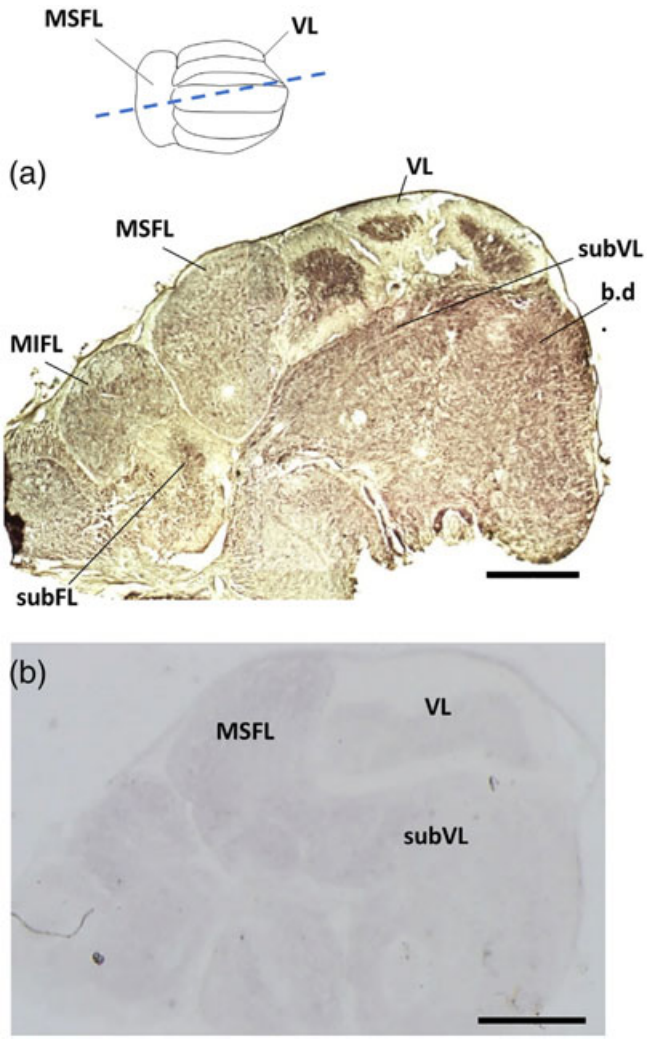

FIGURE 5 *Octopus vulgaris*, light micrograph showing immunohistochemical staining for cChAT in the supraesophageal lobes of the brain. (a) Low magnification of a stained semi-sagittal section of the supraesophageal brain mass (more than one lobulus is seen) reveals a wide distribution of cChAT immunoreactivity throughout many of the lobes, with a uniquely dense labeling of the VL and subFL inner neuropil (note that only small part of the subFL inner neuropil is included in this section). There is a similar but less intense pattern of labeling in the MSFL and MIFL. Unlike the VL there is no clear difference between the densities of the cell body cortices and the neuropilar structures. (b) Light micrograph of control sagittal section with secondary antibody only. Scale bar: 1 mm

GABA-stained slices, visualized as a thin, continuous darker sheath running at the border between the cell body cortex and the outer neuropil of the MSFL tract (Figure 11c, rectangle).

Dense, punctuated GABA-IR was seen in processes in the middle-inner neuropil plexus, mainly in the medial lobule and medial-lateral lobes (Figure 12b), while the outer neuropil, containing mainly fibers of the MSFL-tract, was scarcely labeled (Figure 12a). Figure 12b shows a transverse section where such GABA labeling in the inner neuropil formed a distinct circular pattern with varicosities or thick granular labeling along the processes. These may represent presynaptic varicosities conveying inhibitory input, possibly to the LN dendrites. Such inhibitory inputs may originate from other LNs, GABAergic AMs (see below), or inhibitory afferents from the subVL, such as "pain fibers" described by Young (1971).

Although physiological finding suggested that the excitatory input to the LNs derives from cholinergic AMs (Shomrat et al., 2011), GABA-IR was clearly seen in the region of the AM cell bodies in the VL cell cortex (Figure 13). While unclear staining of the cell somata hindered verification that some of the AMs are indeed GABA-positive,

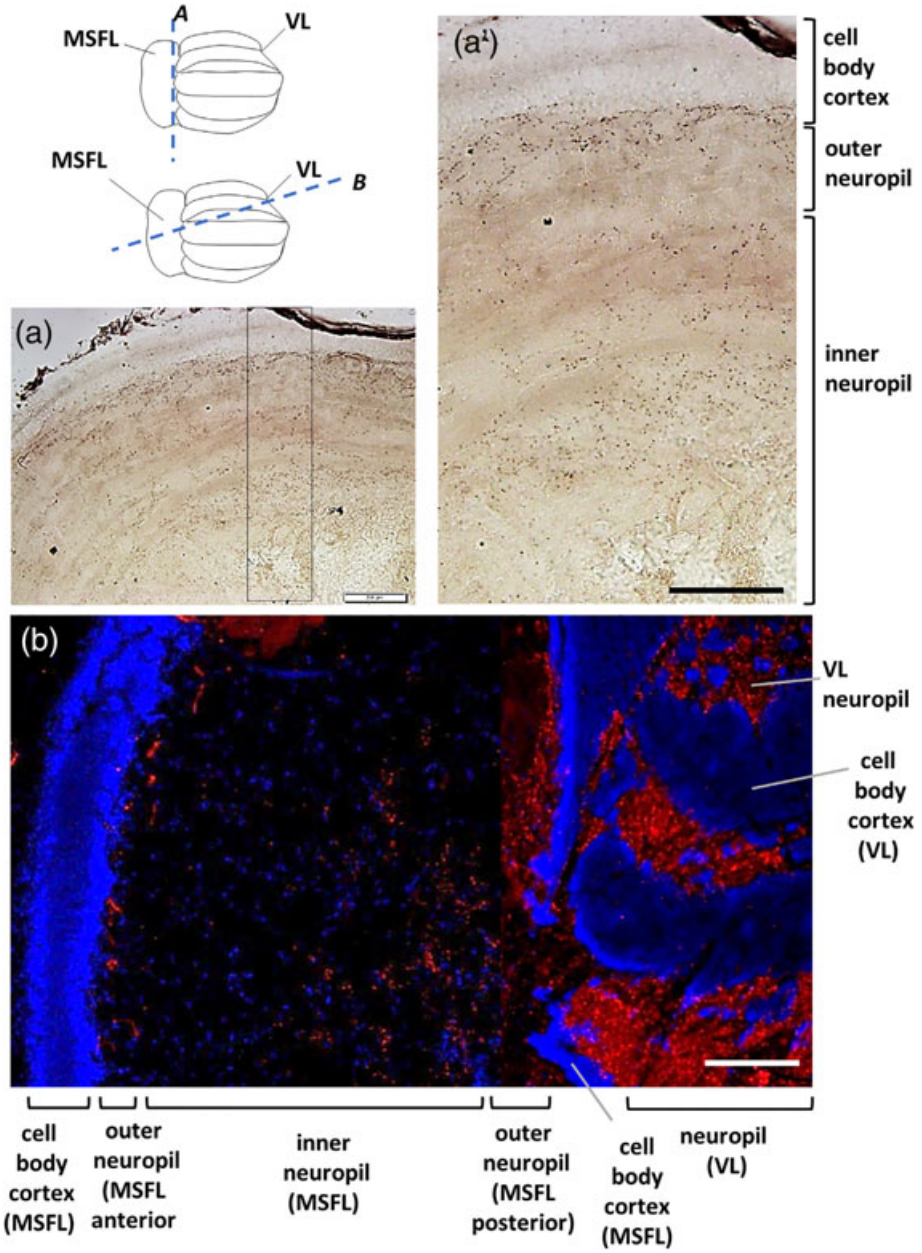

FIGURE 6 *Octopus vulgaris*, cChAT immunolabeling in the MSFL (a) light micrograph of a transverse slice sampled from a posterior region of the MSFL showing from where a' was taken. (a') Some fibrous cChAT-IR labeling can be detected in the MSFL neuropil, where labeling was slightly greater in the outer neuropil and in the center of the medulla where axons from other areas converge. (b) Fluorescent light micrograph of a sagittal-horizontal section showing VL lobuli at the right of the image, revealing similar MSFL cChAT labeling as in a'. The fluorescent labeling is scarce in the middle regions of the MSFL neuropil and slightly more intense in the outer neuropil (anterior and posterior) near the MSFL cell body cortex. Note the abundantly stained VL neuropil (red, cChAT; blue, DAPI). Scale bar: 200 μm

GABA-IR neurite processes were clearly evident running from the AM cell body area and crossing the unlabeled outer neuropil (MSFL tract; Figure 13a,a'). GABA-positive projections crossing the VL hila can be clearly seen in the medial and medial-lateral lobuli (Figure 13b,b', arrowhead).

Support for selected GABAergic AMs was provided by EM-observations in which GABA positivity was detected in what were, most likely, AM neurite bundles and synaptic connections (Figure 14b). Electron microscopy also revealed neuronal processes containing swarms of GABA-IR clear agranular vesicles (*cv*), 30–80 nm dia., associated with amacrine cells (Figure 14c). In some cases, positive synaptic vesicles were seen neighboring unlabeled synaptic terminals (Figure 14d,e). Taken together, these findings show that at least some of the AMs can be GABAergic and thus may provide the inhibitory inputs to the LNs (Shomrat et al., 2011 and unpublished results).

Figure 15a,b shows abundant GABA-IR matrix-like fibrous labeling in the medial inferior frontal lobe (MIFL) similar to that in the MSFL (cf. Figure 10a1). The subFL clearly exhibited large GABA-IR cells distributed in the inner cell body cortex and positive granular processes throughout the neuropil (Figure 15c–e), remarkably resembling the labeling patterns of the VL (Figures 11 and 12).

Using ISH of the metabotropic GABA-B-like receptor mRNA gave especially strong expression in the MSFL cell cortex (Figure 16a). In contrast, there were only some pale expressions in the VL, mostly in the dorsal cell body cortex and in the inner margin of the ventral cell body cortex (Figure 16b, arrows). The cell cortex of the MIFL revealed GABA-B receptor transcript expressions similar to those in the MSFL cell cortex, and the faint expression in the subFL cell cortex corresponded with that in the cell layer of the VL (Figure 16a).

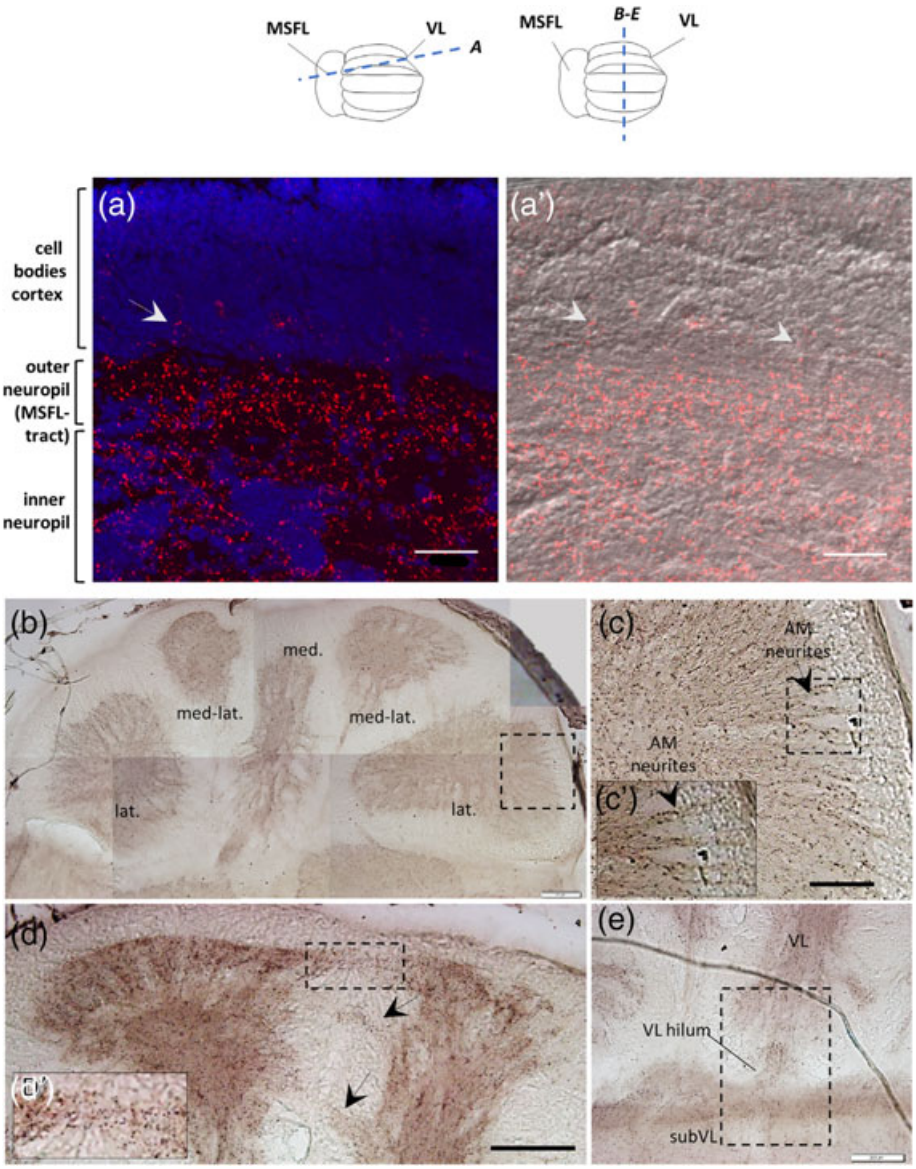

FIGURE 7 *Octopus vulgaris*, distribution of strong cChAT positive labeling in neuronal processes in the VL. (a, a') confocal micrograph showing that the fluorescent signal of the processes in the VL neuropil can be followed vertically into the cell body cortex (arrows). Scattered punctate labeling in the outer cell layers is not of distinct cell bodies counterstained with DAPI (red, cChAT; blue, DAPI). (1:500). (a') Differential interference contrast (DIC) of the cell body cortex and VL neuropil merged with the fluorescent signal (excluding DAPI) of the image in a. (b) Transverse slice of the VL shows the cChAT neuropil labeling is distributed evenly throughout the five lobuli. Marked region indicates area enlarged in c (1:15,000). (c) Abundant cChAT immunoreactivity of processes most likely belonging to bundled AM neurites running vertically (example of three labeled neurite bundles are shown in inset c′). These bundles cross the apparently unlabeled MSFL tract with gaps of ~25–30 μm between them to pass into the neuropil. (d) cChAT-IR along inter-lobule connections between medial and medial-lateral lobuli in a transverse section (marked region and others marked with arrows), suggesting a cholinergic feed among the different lobuli. (1:15,000). (d′) Enlargement of the marked area of crossing fibers. (e) Fibrous cChAT-IR crossing the VL hilum between the VL and the subVL in a transverse section (1:15,000). 50 μm (a, a'); 200 μm (b, e); 100 μm (c)

3.2 | Putative neuromodulators

3.2.1 | Recruitment of NO in the synaptic plasticity pathways

Fixative resistant NADPH-diaphorase reactivity is a reliable marker of NOS activity in molluscan preparations (Moroz et al., 2005; Floyd et al., 1998; Moroz et al., 1999). Fitting with the involvement of NO in LTP in the *Octopus* VL (Turchetti-Maia et al., 2018), intense NADPH-d staining revealed NOS activity in the neuropil of all five VL lobuli (Figure 17a,b,c1,c2) and in the subFL (Figure 17a,e). In the VL, staining was found in the inner zones where the synaptic connections between the AM and the LNs lie. The outer neuropil was more sparsely stained, probably because in this region unlabeled axons that run in the MSFL tract make sparse *en passant* connections with AM neurites. The AM neurites can be seen crossing the tract in faintly stained AM trunks with gaps of 2–10 μm between them (arrows Figure 17d1), suggesting the presence of NOS in the AM neurites. The patterns of labeling in the VL and the subFL were highly similar (Figure 17d1,d2). Note the clear but sparse labeling of cell bodies in the subFL cortex (Figure 17f, arrows).

The MSFL neuropil also contained NADPH-d positive processes (Figure 17e), although staining was much less abundant than in the VL and subVL (Figure 17a). Staining was distributed throughout most of the MSFL neuropil, especially at a thin layer below the cortex. Scarce labeling was seen in the plexiform arrangement in the deeper central region of the lobe (Figure 17e), an area containing mainly incoming fibers (Young, 1971).

3.2.2 | Catecholaminergic system: Tyrosine hydroxylase

Tyrosine hydroxylase (TH)-positive labeling showed prominently in a group of neurons with large cell bodies (>10 μm dia.) in the posterior MSFL lobe, bordering, or possibly belonging to, the VL

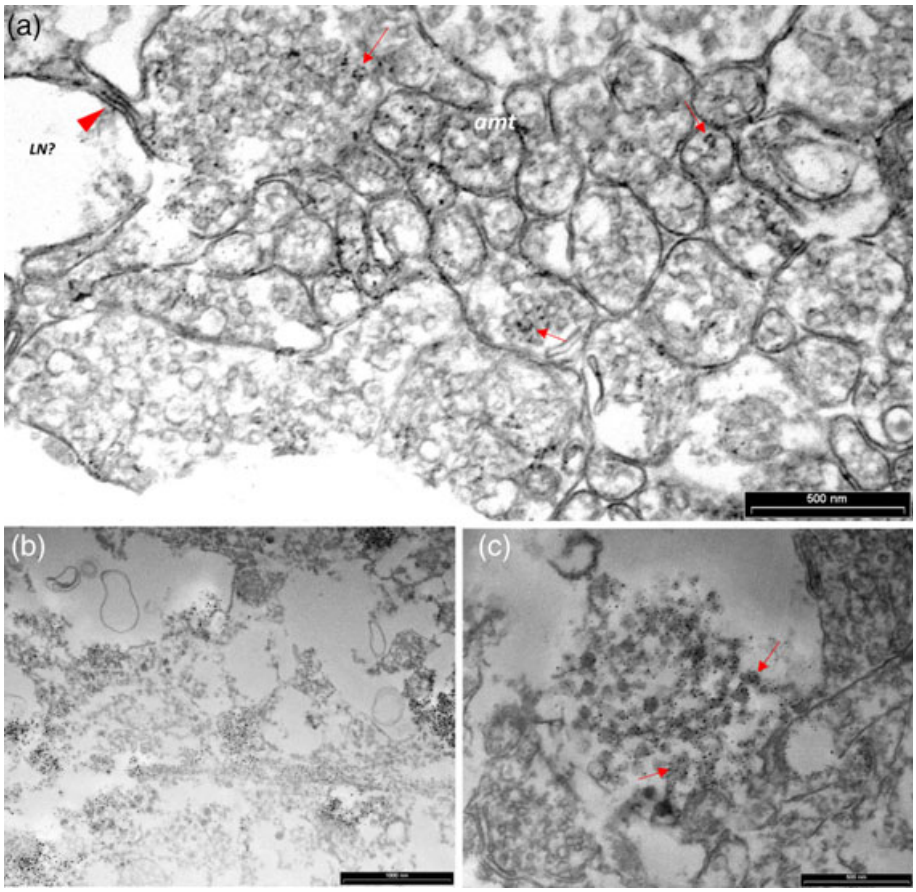

FIGURE 8 *Octopus vulgaris*, cChAT immuno-EM of neuronal profiles in the VL neuropil. (a) Electron micrographs showing cChAT-IR in agranular vesicles in profiles typical for amacrine trunks (*amt*) (arrows) in the inner neuropil (cut transversely). Note a pale unstained non-vesicular profile, possibly a LN (*LN?*), shows a synaptic connection density (thickened membrane, red arrowhead) with one of the positively stained trunks. (b) Fairly widespread cChAT immunoreactivity is possibly distributed in synaptic structures and processes in the neuropil mass. While it is not fully clear to which cells the labeled structures belong, neighboring profiles remain unlabeled. (c) Electron micrograph showing intensely labeled dark granulated vesicles of various sizes (arrows), which are probably not to be attributed to MSFL incoming fibers. Scale bar: 500 nm (a, c); 1000 nm (b)

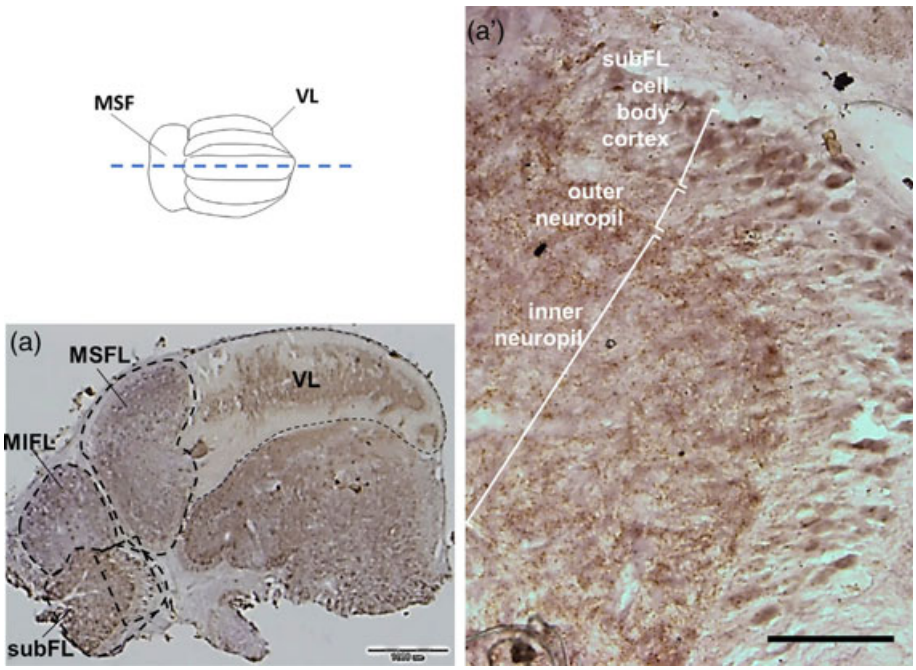

FIGURE 9 *Octopus vulgaris*, cChAT-IR distribution in the MIFL-subFL touch learning system. (a) Sagittal section from the middle area of the supraesophageal brain. Dotted rectangle gives the location of section a'. Note the similarity in intensity patterns of the MIFL and MSFL and in the intense, brownish labeling of the inner neuropil in VL and subFL (1:15,000). (a') Enlarged area of cell bodies and neuropil of the subFL. There is positive labeling of relatively large cell bodies (>20 μm) localized in the outer cell cortex (top bracket). This location differs from that of the LNs mainly organized in the outer layers in the VL cell cortex. The MIFL-tract is barely apparent in this section (middle bracket), and dense labeling of processes is uniformly distributed in the inner neuropil (lower bracket). Scale bar: 1 mm (a); 200 μm (a')

(Figure 18a,b). This cluster formed a "deep nucleus," contrasting with the regular organization of cell bodies in an outer cortex. TH-IR could be followed for some distance in neuronal processes (Figure 18a"). Similar cells, in a similar location, also showed L-glutamate-IR (Figure 5), and formed symmetrical tree-like structures feeding into the anterior region of the VL neuropil (Figure 18a,a'). Only few TH-positive large cells (~12.5 μm dia.) were detected in the VL cortex; these lay in the inner margin of the VL

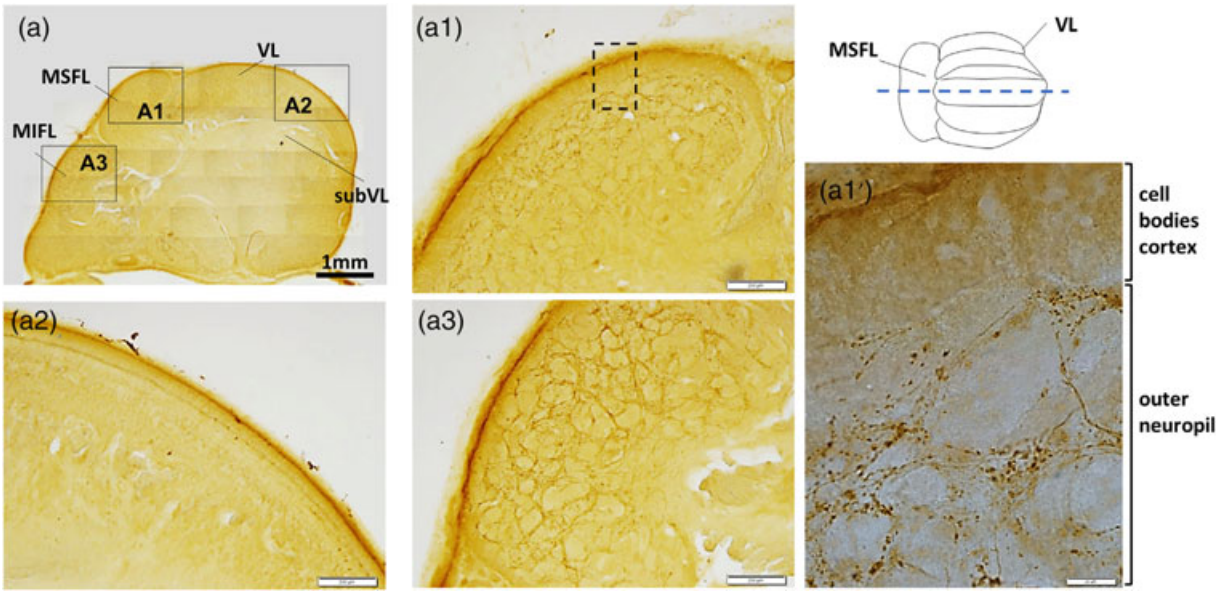

FIGURE 10 *Octopus vulgaris*, light microscopic micrographs of sagittal sections showing GABA-immunoreactivity labeling in supraesophageal lobes of the brain. (a) Low magnification of supraesophageal brain preparation labeled for GABA, showing the MSFL (a1), VL (a2), and MIFL (a3) where specific labeling patterns were identified. (a1') High magnification of the area marked in a1 showing GABA-IR labeling in the MSFL. No specific labeling was detected in the cell body cortex as opposed to the rich GABAergic area in the outer neuropil of the MSFL lobe with GABA-positive processes with dark varicosity-like labeling. GABA-positive processes and varicosities are scarcely detectable in the inner neuropil. Dark labeling of the sheath surrounding the brain and general faint staining was not observed in controls with secondary antibodies only (not shown). Scale bar: 1 mm (a); 200 μm (a1–a3); 20 μm (a1')

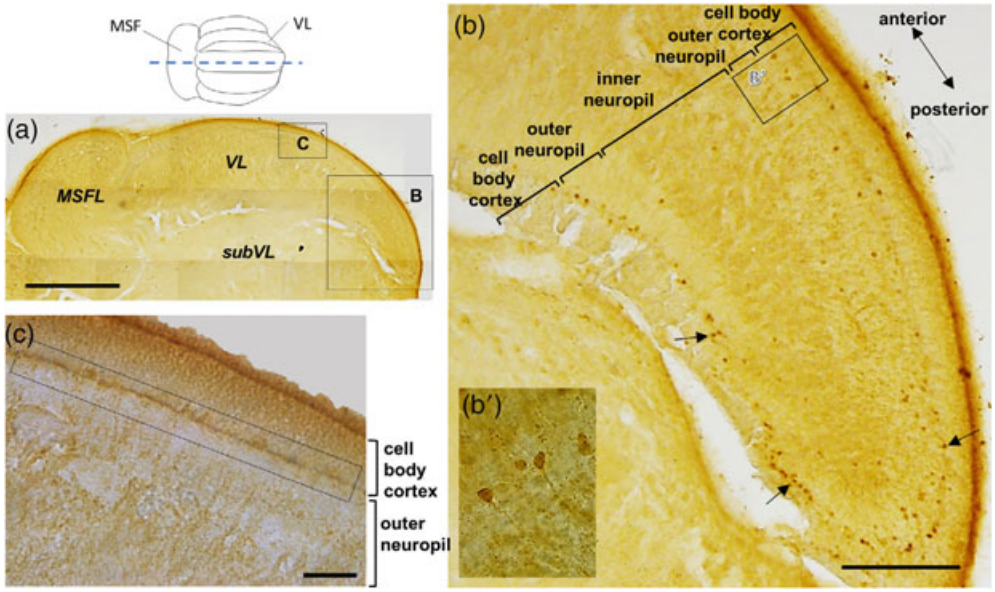

FIGURE 11 *Octopus vulgaris*, light microscopic micrographs showing GABA-IR of large cell bodies in the VL. (a) Low magnification of the MSFL-VL system in a GABA-positive labeled sagittal slice, with locations of b and c marked. (b) The location and organization of GABA-IR large cell bodies (dia. 6–13 μm; arrows) around the inner dorsal and ventral margin of the cell body cortex strongly suggest that these are LNs. (b′) Higher magnification of individual GABA-IR large cells showing their positively labeled neurites emerging toward the inner neuropil, further indicating that these are "classical" LNs. (c) A thin, anatomically yet undefined, dark layer runs along the border between the inner cell layer and the outer neuropil (rectangle). Scale bar: 1 mm (a); 200 μm (b); 50 μm (c)

cell cortex, where the LNs lie. Their projections also showed positive TH labeling and could be followed inward to the depth of the VL neuropil (Figure 19a', arrows). It is not yet clear if these dopaminergic (or other catecholamines) neurons are special efferent LNs or constitute an internal neuromodulatory system (see below).

TH immunoreactivity was evident in both the inner and outer VL neuropil. The outer neuropil showed TH-positive processes interweaving in the lower part of the cell layer (Figure 19b,b' arrows, Figure 20a), while in the dorsal and ventral aspects of the inner neuropil a dark TH-IR impressively defined a thickened band carrying TH-positive fibers with varicosities along their length (Figure 20a). Correspondingly, ring-like thickenings were seen in transversal sections (Figure 20b,b'), suggesting dopaminergic innervation of a specific dendritic area of, for example, an LN. These ring-like patterns in the central inner neuropil and the VL-subVL crossing fibers were evident mainly in the medial and medial-lateral lobuli, while only scarce TH-IR fibers were seen crossing through the VL hila of the lateral lobuli. The spatial distribution of the TH-IR at the center of the inner VL neuropil suggests that the source of some of the labeled twigs may be afferent processes from ventral lobes originating or crossing through the subVL to the VL. Additional sources for these processes are the TH-positive cells organized as a "deep nucleus" at the MSF-VL border (Figure 18) and the TH-IR LN in the VL cell cortex (Figure 19a).

3.3 | Predicted neuropeptides

The expressions of some well documented molluscan neuromodulatory neuropeptides, such as FMRFamide-like neuropeptides (FLPs), buccalin, bradykinin and conopressin peptide were localized in the VL using ISH (Figures 21 and 22 and see (Winters, 2018). FLRIamide-encoding transcript expression (Figure 21a1,a2) was distributed in a distinctly organized pattern, clearly highlighting large cells bodies dispersed uniformly in the inner margin of the cortex in all five lobuli where the LNs lie and where GABAergic and glutamatergic LNs were found. The unique pattern of labeled cells expressing FLRIamide transcripts suggests that at least some of the LNs express FMRFamide-related peptide (FaRP) as a cotransmitter in addition to their conventional fast transmitters.

FMRFamide mRNA expression was seen in the MSFL at the ventral areas of the VL lobuli, MIFL and subFL. Cell expressions of FMRFamide-encoding transcripts were more widely distributed in other supraesophageal lobes, including the subVL (Figure 21b1,b2).

Buccalin mRNA was identified in the inner margin of the VL cell body cortex but not in the MSFL (Figure 22a1,a2). As reported in (Winters, 2018) cells expressing bradykynin mRNA were found in the VL cell cortex, but not in the MSFL (Figure 22b1,b2). Cell bodies expressing bradykinin were also scattered in inner areas of the VL, in what appeared to be cortical folds between lobuli. Like FLRIamide-encoding transcript, bradykynin and especially buccalin mRNA seem to be expressed in the internal margin of the VL cortex suggesting that these neuropeptides are cotransmitters of the LNs. Conopressin mRNA was expressed in cells throughout the cell body cortex of the

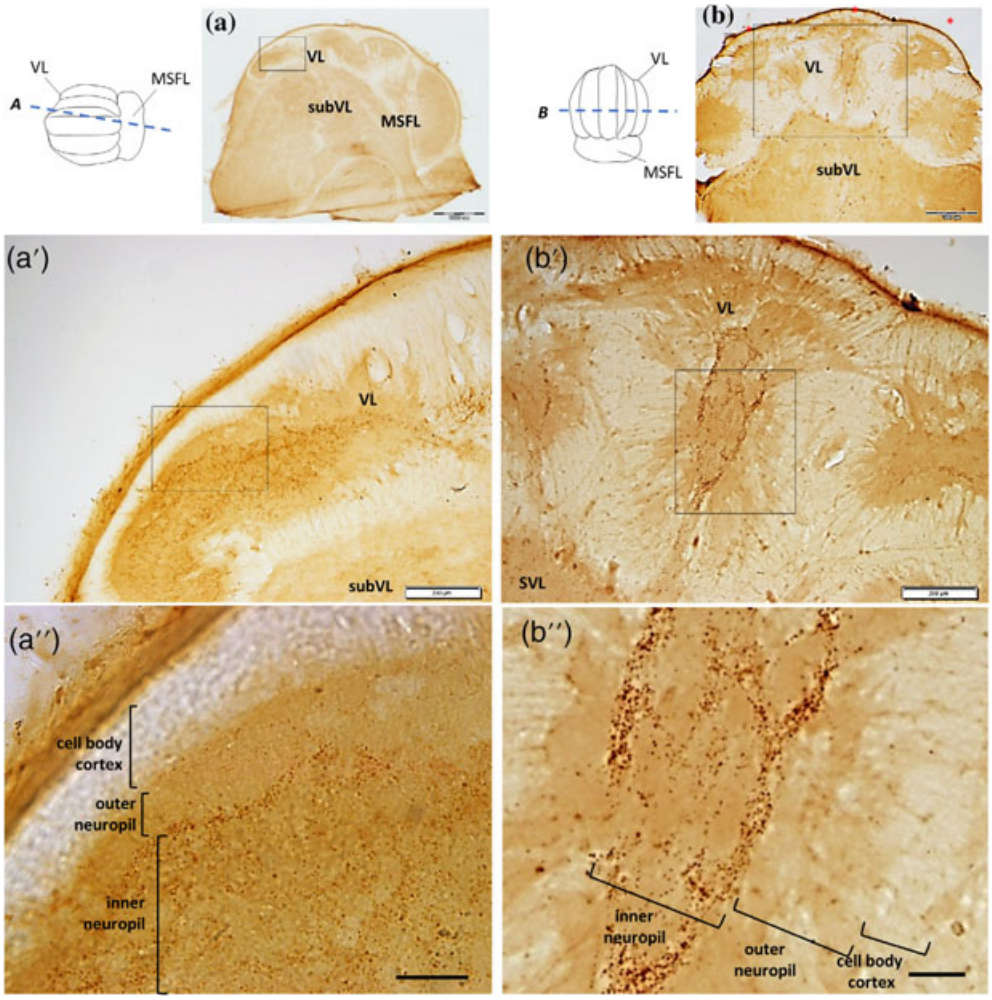

FIGURE 12 *Octopus vulgaris*, GABA-IR reveals a unique dense labeling pattern in a distinct area in the inner neuropil. (a) Low magnification of a semi-sagittal slice labeled for GABA, including the MSFL-VL system. Location of a' is marked. (a') GABA-IR labeling in the inner neuropil. (a") Higher magnification of the area marked in a' showing barely noticeable GABA-IR in the AM cell layer and in the outer neuropil (MSFL-tract), while punctuated dark labeling is seen in the inner neuropil. (b) Low magnification of a transverse slice labeled for GABA, including the five VL lobuli. (b′) Enlargement of the area marked in b. The GABA-IR observed in transverse section forms a distinct loop-like pattern in the inner neuropil. (b″) Enlargement of the area marked in b′ shows that the dense labeling carries varicose-like markings suggesting this area comprises GABAergic synaptic terminals. Scale bar: 1 mm (a); 500 μm (b); 200 μm (a', b′), 50 μm (a", b″)

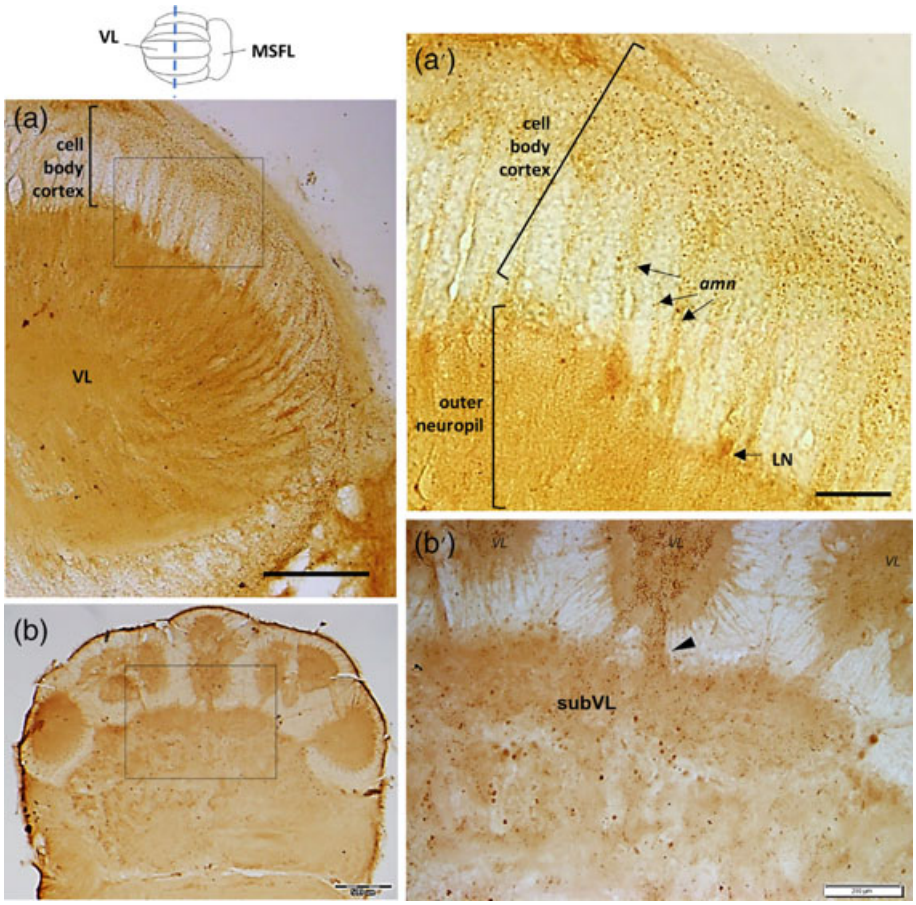

FIGURE 13 *Octopus vulgaris*, light microscopic micrographs show GABA-positive processes crossing the cell body cortex within and outside the VL. (a) Low magnification of a transverse section of a lateral lobule labeled for GABA. The location of a' marked is. (a') Higher magnification of a lateral lobule showing GABA-IR in bundles of processes crossing the apparently unlabeled MSFL axons in the outer neuropil with consistent gaps of approximately 20 μm between them (arrows). These processes appear to reach both outer cell layers and the VL neuropil and are most likely AM neurites (*amn*). Large cells positively labeled for GABA are situated in the inner margin of the cell layer cortex (arrow). (b) Low magnification of a transverse section of the supraesophageal brain. Location of b′ is marked. (b′) GABA-IR in processes (arrowheads) connecting the VL with subVL. Scale bar: 200 μm (a); 50 μm (a'); 500 μm (b); 200 μm (b′)

VL lobules, especially in the lateral lobules (Figure 22c1,c2). In contrast to the scattered distribution of bradykinin and conopressin mRNAs in the VL, these transcripts were expressed in district areas of other regions of the brain.

Myomodulin peptide mRNA was expressed in cells at the MSFL-VL border (Figure 22d), seemingly belonging to the cell bodies in the "deep nucleus" (see Figures 4 and 18). Some positively labeled cells were also seen at the VL ventral cell cortex-subVL border.

4 | DISCUSSION

Cephalopods traced their ancestry to the early Cambrian (~522 million years ago) at the very beginning of the explosive radiation of bilaterian bodyplans (Hildenbrand et al., 2021). Thus, their rise and evolution had been paralleled by the burst of diversification of arthropods and chordates (Erwin & Valentine, 2013). Starting from the dawn of their evolution, cephalopods successfully competed with arthropods and vertebrates in ancient seas Packard 1972. As a result, such ecological competition with other top predators (especially with vertebrates over the whole evolutionary time-scale—e.g., Hoffmann et al., 2020) led to the independent origins of multiple complex innovations in cephalopods' homeostatic, circulatory, locomotory (Nesher et al., 2020), sensory, and neural systems (Moroz, 2009; Nieder, 2021; Albertin, Simakov, 2020; Yoshida et al., 2015; Di Cosmo et al., 2021; Fuchs et al., 2021).

Co-option of developmental programs in the neural and sensory and molecular receptor specification further emphasizes the uniqueness of cephalopod innovations (Yoshida et al., 2015; Neal et al., 2022; Moroz et al., 2021). Independent centralization of cephalopod neural systems (Moroz, 2009; Hochner & Glanzman, 2016) also led to convergent development of elementary cognition and higher neuronal functions (Schnell et al., 2021; Mallatt & Feinberg, 2021), including the formation of elaborated learning and memory centers such as vertical lobes (Young, 1971, 1991) with unique microanatomical and molecular organization as we discuss below.

The VL is arranged as a matrix in a fan-out fan-in network configuration (see Figure 1c), in which the incoming MSF axons innervate *en passant* a large group of minute amacrine interneurons (AM). These, in turn, converge onto a relatively small group of large efferent neurons (LNs; Gray, 1970; Young, 1971). Physiological experiments revealed an excitatory feedforward connectivity in which MSF afferents connect to the AMs via excitatory glutamatergic-AMPA-like receptor type synapses (Hochner et al., 2003), while the AMs show converging cholinergic excitatory synaptic connections to LNs (Shomrat et al., 2011). Plasticity is expressed as a robust activity-dependent LTP at the glutamatergic MSFL-AM connections (Hochner et al., 2003). This LTP is important for behavioral learning and the acquisition of long-term memory (Shomrat et al., 2008).

Even after decades of study, the neuroanatomical distribution of neurotransmitters and neuromodulators of the learning and memory

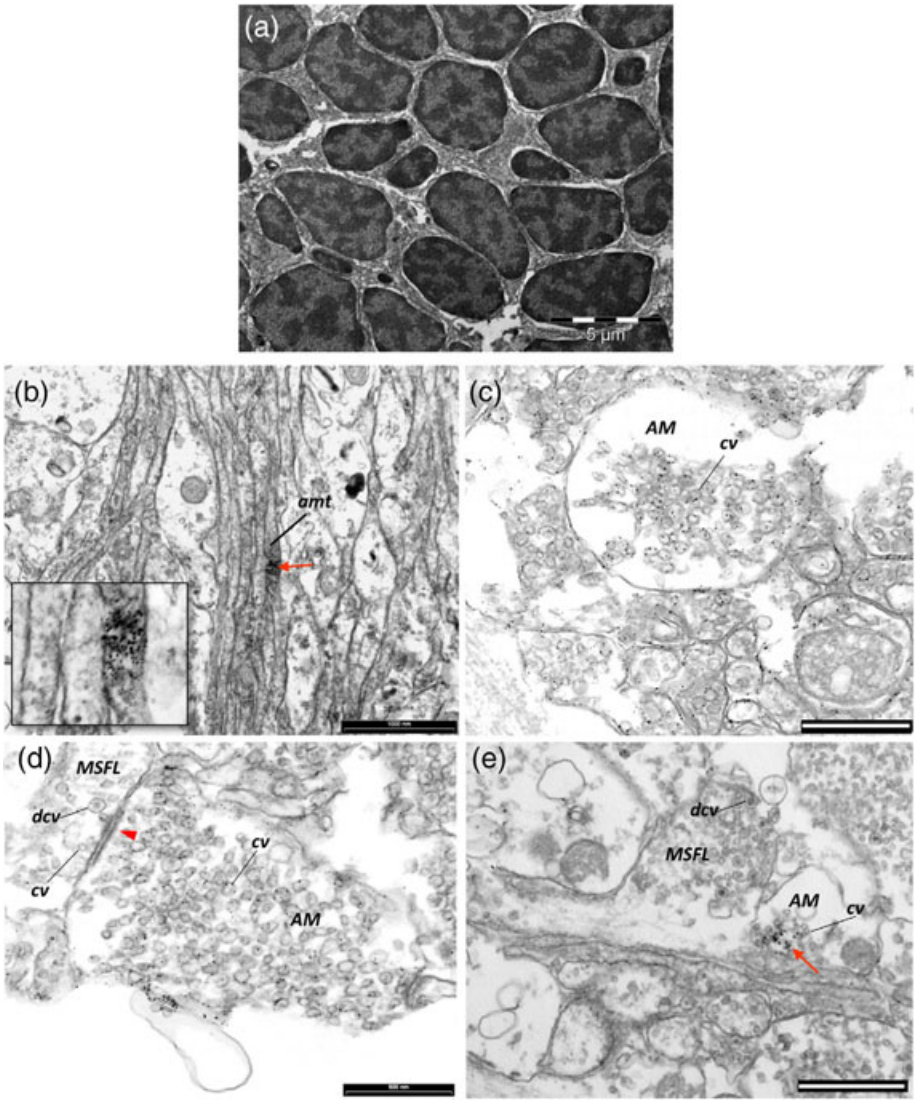

FIGURE 14 *Octopus vulgaris*, transmission electron micrographs showing GABA-IR in the VL. (a) Section showing the closely packed cell bodies of the small AMs. The nucleus occupies most of the cell body. (b) A longitudinal section in the outer neuropil. Although GABA-IR was not identified in the cell body cortex, labeling was observed in a process (red arrow) crossing over MSFL axons. (c) Section of an ovoid varicosity. GABA-IR can be seen in agranular clear vesicles (cv), associated with AMs ranging from 30 to 80 nm dia. (d) Neighboring cells sampled from the outer neuropil area. The cell containing cv (probably AM) reveals GABA-IR, while no labeling was identified in the adjacent MSFL varicosity containing cv and dense core vesicles (dcv). Note the membrane thickening (arrowhead) suggests a synaptic contact between the two but without clear directionality. (e) GABA-IR in cv docked near the membrane of a cell neighboring an MSFL axon synapse, which hints at inhibitory synapses in the area of the MSFL axon terminals. Scale bar: 5 µm (a); 1 µm (b, e), 500 nm (c, d)

system of the octopus VL remained elusive. This study, therefore, aimed to better understand the VL system, mainly motivated by the notion that neurons should be classified into cell types not only by location and shape but also according to their neurotransmitter, neuropeptides, and neuromodulators. Some of our results fit the physiological models (e.g., glutamatergic MSFL neurons, cholinergic AMs, GABAergic LNs). At the same time, other findings are novel (e.g., putative GABAergic AM) and suggest that the apparently simple input–output relationship of the VL is mediated by a more complex network than the fan-out fan-in feedforward excitatory connections found previously (Shomrat et al., 2011).

4.1 | MSF fiber inputs to the VL via L-glutamate synapses

ISH revealed VGLUT-encoding mRNA in the cell body cortex of the MSFL (Figure 2a), supporting L-glutamate (L-Glu) as the transmitter for these neurons. Immunolabeling of L-Glu (Figure 3) revealed especially densely labeled varicosities, such as those localized at the lower margin of the MSFL tract where the MSFL terminals synapse with the AM neurites (Gray, 1970). These results support the physiological findings of glutamatergic connectivity at the first VL input fan-out synaptic layer (Hochner et al., 2003; Shomrat, et al., 2011). No VGLUT labeling was seen in the VL cell cortex, suggesting that the majority of the cells in the VL (e.g., AMs) use different neurotransmitters from the MSFL.

4.2 | AMs input to LNs via cholinergic and GABAergic synapses

Specific cChAT labeling was seen in the AM neurites, with especially strong immunoreactivity in the inner neuropil, the site of the serial synapses of amacrine cells with LNs (Gray, 1970; Shomrat et al., 2011). The cholinergic processes were restricted to the inner neuropil region, emphasizing an evenly distributed cholinergic

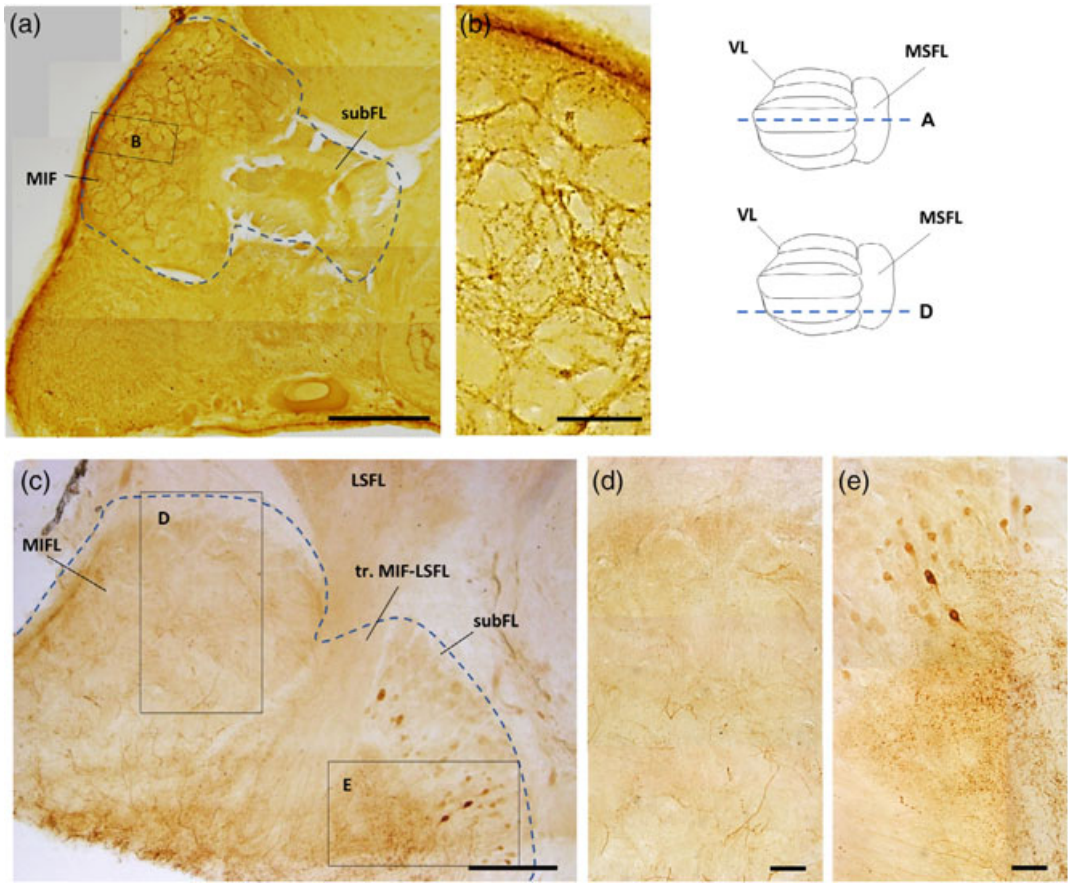

FIGURE 15 *Octopus vulgaris*, GABA-IR distribution in the touch learning system. (a, c) Sagittal GABA-labeled sections of the MIFL-subFL. Marked areas are shown at higher magnification in b, d, and e. (b) Prominent labeling of the MIFL neuropil comparable to the labeling pattern in the MSFL (see Figure 10). (d) A more lateral section in which the labeled processes are still apparent but less intense. (e) The subFL mass clearly demonstrates large cell GABA-IR in the inner cell body cortex and positive labeling of the neuropil mass comparable to the labeling patterns in the VL (see Figure 11). Scale bar: 500 μm (a); 100 μm (b–e)

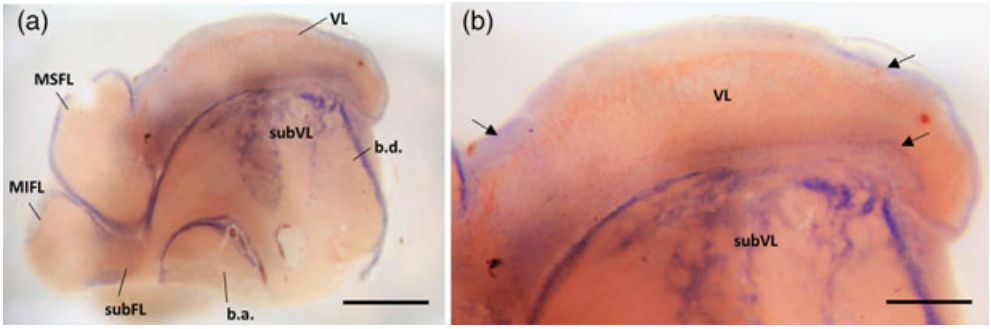

FIGURE 16 *Octopus vulgaris*, micrographs of GABA-B expression detected by in situ hybridization in supraesophageal lobe sections. (a) Cells strongly expressing GABA-B mRNA can be seen in the MSFL cell cortex, subVL, and the basal lobes. (b) Higher magnification of the VL reveals faint expressions of GABA-B mRNA in the cell body cortex of the VL. The VL and the subFL appear to express lower levels of GABA-B receptors than the other lobes. Scale bar: 1 mm (a); 500 μm (b)

innervation in the dendritic area of the input to the LNs (Figures 6 and 7). These results confirm the physiological findings of cholinergic AM-to-LN synapses (Shomrat et al., 2011).

Synaptic plasticity in this learning network occurs at predicted glutamatergic connections between the MSFL axon terminals and the AMs. Yet, in the related cuttlefish (*Sepia officinalis*), the plasticity occurs in the second layer, where ACh is likely the excitatory transmitter (Shomrat et al., 2011). This dichotomy suggests that, in cephalopods, the molecular mechanism of LTP is not associated with a single specific neurotransmitter.

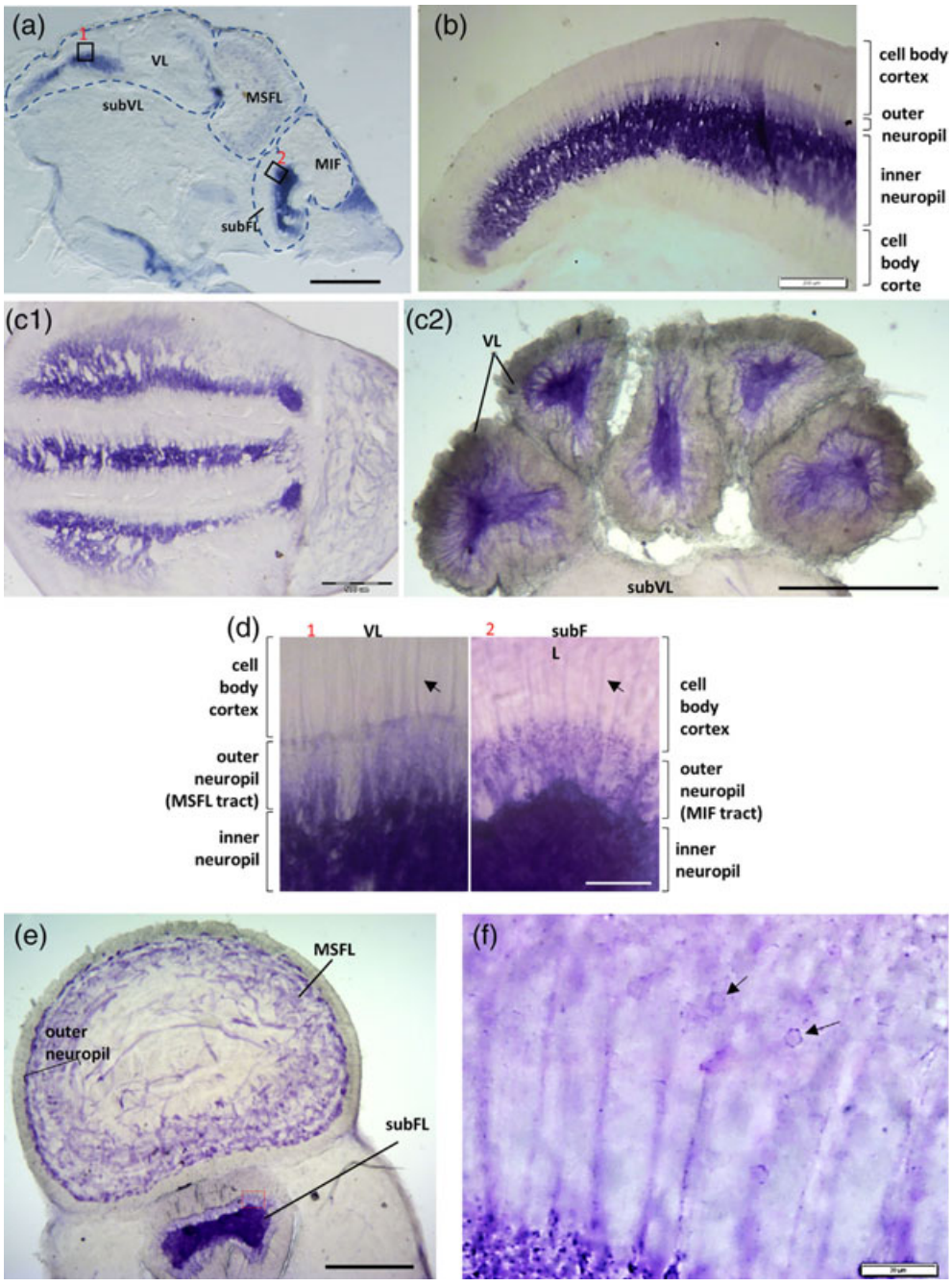

FIGURE 17 *Octopus vulgaris*, intense NOS activity in the MSFL-VL and MIFL-subFL systems revealed by NADPH-d labeling in the supraesophageal lobes. (a) Sagittal section with intense labeling of the neuropil in VL and subFL. (b) NADPH-d labeling in the VL showing different staining patterns in the cell body cortex, outer and inner neuropil. (c1, c2) Horizontal (c1) and transverse (c2) sections of the VL lobuli showing a similar pattern of positive NADPH-d labeling in the different lobuli. (d) Higher magnification of the areas marked in (a) showing comparable labeling patterns between brain structures involved in visual learning (VL) and tactile learning (SuFL) systems. (e) Transverse section of the MSFL and subFL area showing positive labeling. In the MSFL the staining in the outer neuropil is darker than in the center. (f) Enlargement of area marked in e (subFL) showing positive NADPH-d neurites and cell bodies (arrows). Scale bar: 500 μm (a, c1, c2, e); 200 μm (b); 50 μm (d); 20 μm (f) [figures a,c2, d from Turchetti-Maia et al., 2018]

Morphologically the AMs appear to make up a largely homogeneous population (Gray, 1970; Young, 1971). Yet, while some AM are cholinergic, we found that some AMs could be GABAergic (Figures 13 and 14). The proposed transmitter diversity of AMs may explain previous findings that stimulation of the MSFL tract evoked IPSPs in some LNs (Shomrat et al., 2011). Thus, the AMs appear to be functionally and chemically heterogeneous. Indeed, an ongoing connectome study (Bidel et al., 2021) has been able to divide the AMs into two distinct groups. More than 95% are "simple" AMs, receiving synaptic input from MSFL neurons and sending a single non-bifurcating neurite into the neuropil. The remaining AMs are "complex," seeming to integrate inputs from several MSFL neurons and several simple AMs, their neurites bifurcating extensively in the outer neuropil at the level of the MSFL tract where they receive inputs from the SFL axonal varicosities. These processes run into the inner neuropil, where they innervate LNs processes. It is reasonable to propose that some interneurons are inhibitory and thus stained positively for GABA. It remains to be clarified whether this population of inhibitory AMs is the group of complex AMs discovered in the EM study (Bidel et al., 2021).

The restriction of the GABAergic varicosities to the inner neuropil, mainly in the medial and medial-lateral lobuli (Figure 12), indicates that dendritic branches may compartmentalize GABAergic signaling in general or, particularly, inhibition. If these GABAergic varicosities

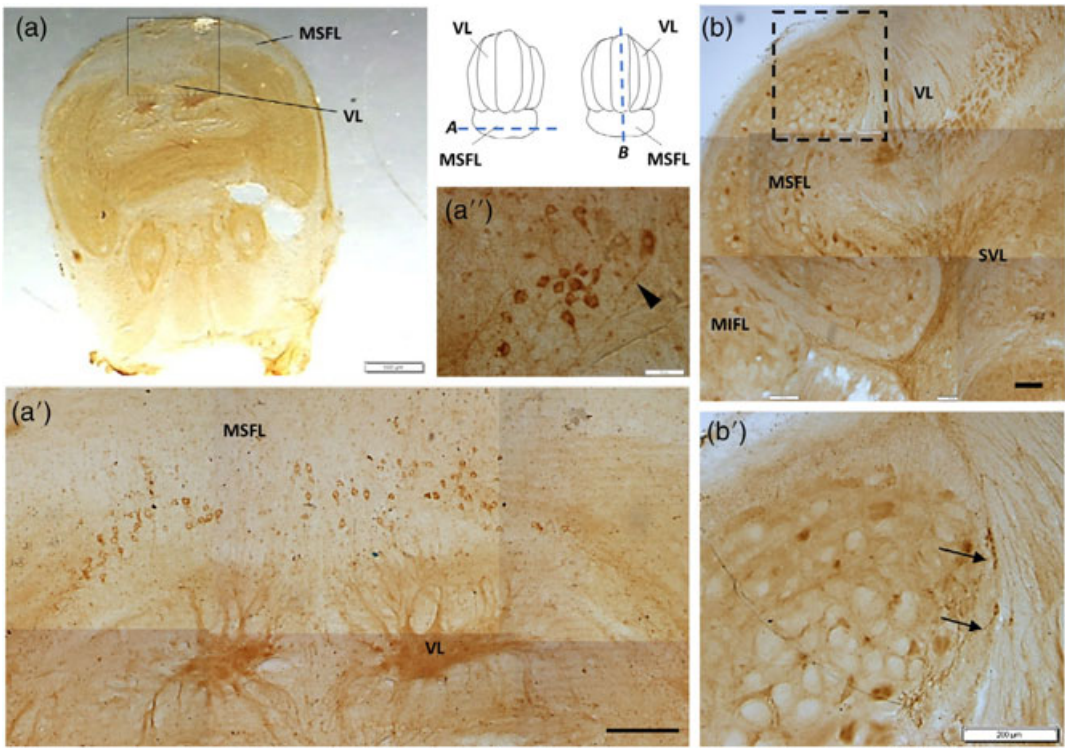

FIGURE 18 *Octopus vulgaris*, tyrosine hydroxylase (TH) immunoreactivity reveals a "deep nucleus" in the VL-MSFL system. (a) Transverse TH-labeled slice from the border area between the MSFL and the VL. The location of a' is marked. (a') Grouped TH-IR cell bodies localized in the anterior VL area/posterior MSFL organized as a "deep nucleus" (cell dia. ~16–20 μm). (a") TH-IR projections from cells localized in the deep nucleus can be followed a certain distance (arrowhead; image from slice similar to a). (b) TH-labeled sagittal slice of the MSFL and neighboring areas. Location of B′ is marked. (b′) Higher magnification showing several cells that probably belong to the "deep nucleus" (arrows). Scale bar: 0.5 mm (a); 200 μm (a', b, b′); 50 μm (a")

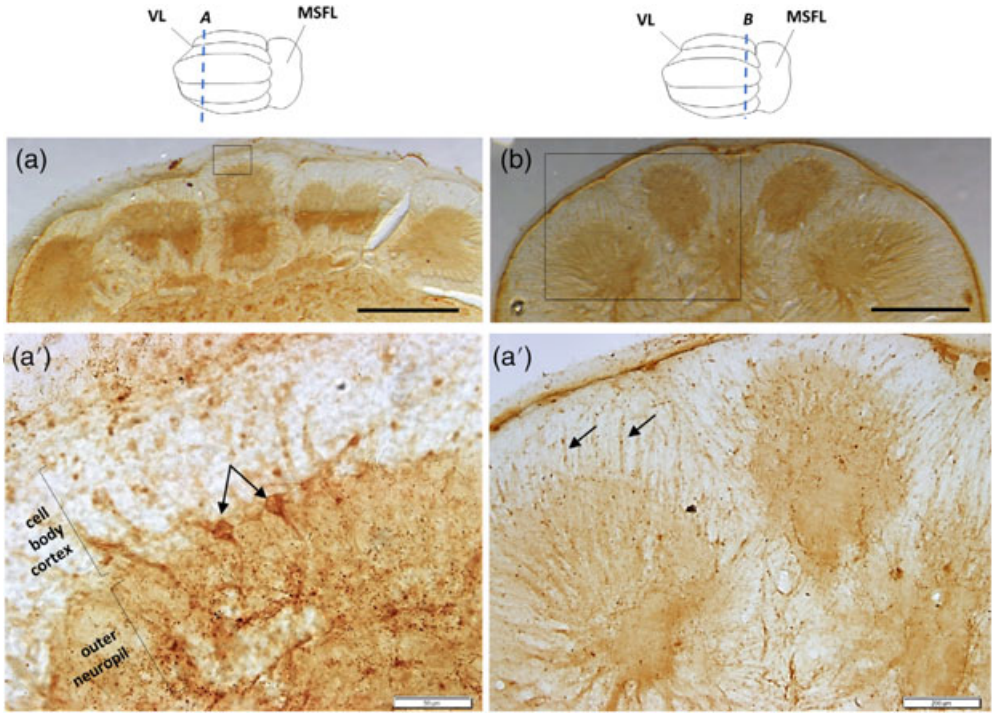

FIGURE 19 *Octopus vulgaris*, scarce TH immunoreactivity in the cell body cortex of the VL. (a, b) Transverse TH- labeled slices. Locations of a' and b′ are marked. (a') TH-positive large cell bodies (~13 μm dia.) located in the inner layers of the VL cell cortex. They project inwards to the neuropil. (b′) Transverse view of part of the VL lobuli showing faint staining of neuronal processes running between the cell body layers and the neuropil (arrows). There is clear granular labeling in the neuropil (see also Figure 21). Scale bar: 500 μm (a,b); 50 μm (a'); 200 μm (b′)

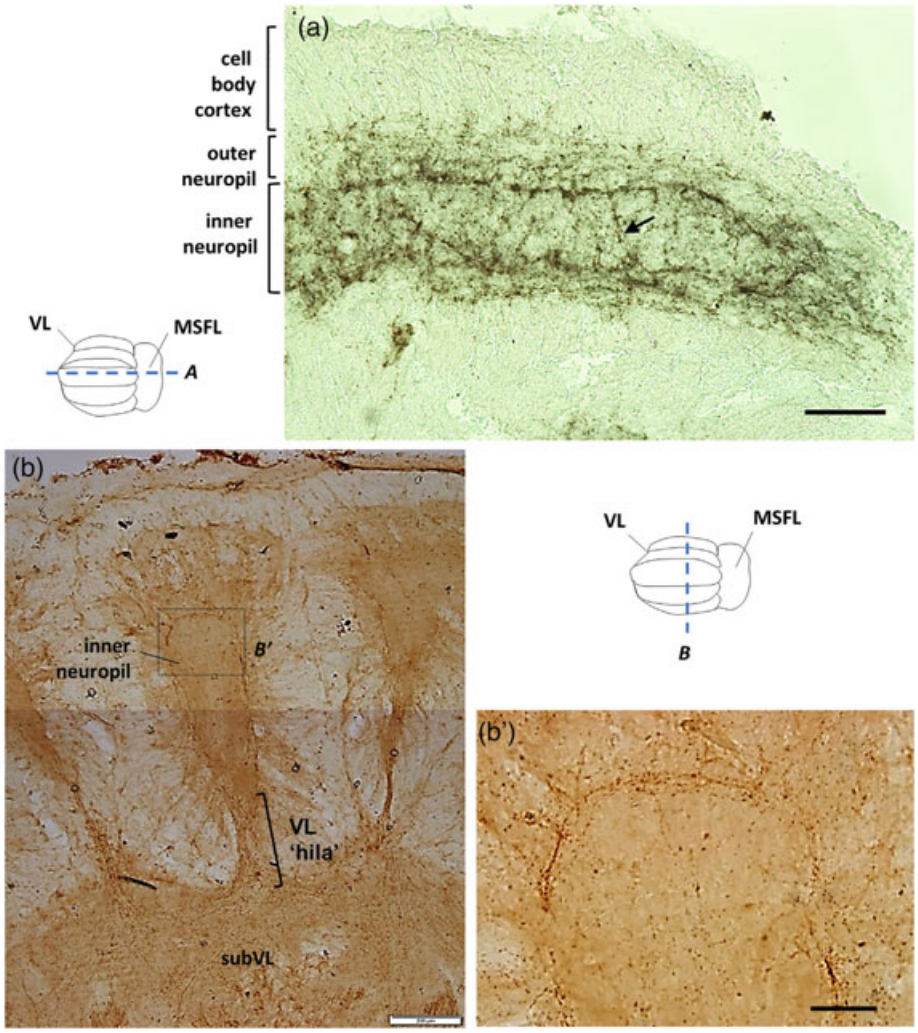

FIGURE 20 *Octopus vulgaris*, TH-immunoreactivity in the VL neuropil. (a) A sagittal slice of the VL showing TH-IR in both the inner and outer neuropil but no clear TH-IR cell bodies in the AM cell body layer. The inner neuropil is characterized by an impressively defined TH-IR ring-like band carrying positively stained thickenings and varicose fibers along its length. (b) The TH-IR ring-like labeling in the inner medial lobule neuropil (transverse section) corresponding to the labeling in (a). TH-IR processes in subVL-VL tracts crossing the VL hila were observed mainly in the medial and medial-lateral lobes. Note the bottleneck-like morphology where the labeling is especially dense (brackets). Location of b′ is marked. (b′) TH-IR dense ring-like labeled processes in the inner neuropil. Scale bar: 200 μm (a, b); 50 μm (b′)

originate from GABAergic AMs, the proposed GABA-mediated inhibition may provide a feedforward inhibition of LNs. An immunohistochemical study in *Octopus bimaculoides* suggested that serotonin is distributed unevenly in the five lobuli indicating functional differentiation among them (Shigeno & Ragsdale, 2015). In our study, the uneven distribution of GABAergic varicosities in the five lobuli was the most indicative result supporting further functional differentiation among the VL regions and their neurons.

4.3 | Heterogeneity and co-transmission of the LNs

Strikingly organized GABA-IR LN cell bodies were localized in the inner cortex of the VL (Figure 11), confirming that these neurons can provide the predicted inhibitory output from the VL as previously postulated from staining (Cornwell et al., 1993), lesioning (Boycott & Young, 1955) and behavioral and physiological experiments (Shomrat et al., 2008). This provides support for the VL model in which the output has an inhibitory control over other circuits, such as those for attack behavior (see Turchetti-Maia et al., 2017).

Yet, glutamatergic LNs were also detected in the cell cortex (Figure 3), suggesting that like the AMs, the LNs do not comprise a homogenous population. Even taking into account that glutamatergic-IR may also label GABAergic cells, as glutamate is a metabolic precursor for GABA synthesis (Villar-Cerviño et al., 2013), the distribution and morphological characteristics of the group of glutamate-labeled LN cell bodies seemed to differ from the classic GABAergic LNs.

It is not clear if the axons of these LNs project out of the VL to form a parallel excitatory output that may facilitate behaviors like the attack behavior. Or they could be part of recurrent excitatory connections between the VL and the MSFL forming reverberatory cyclic networks as postulated by Young (1991, 1995). Recurrent reverberatory circuits may subserve working memory by maintaining ongoing electrical activity. Tracing techniques have revealed such possible connections in cuttlefish, though the nature of their transmission system is not yet clear (Graindorge et al., 2008).

LNs, and possibly other large cells in similar areas also express neuromodulatory neuropeptides. The FMRFamide-like neuropeptide, FLRIamide, showed the most prominent labeling pattern in specific VL neurons (Figure 21a). This suggests that, in addition to the fast transmitter GABA, the LNs contain a small neuropeptide FaRP as a

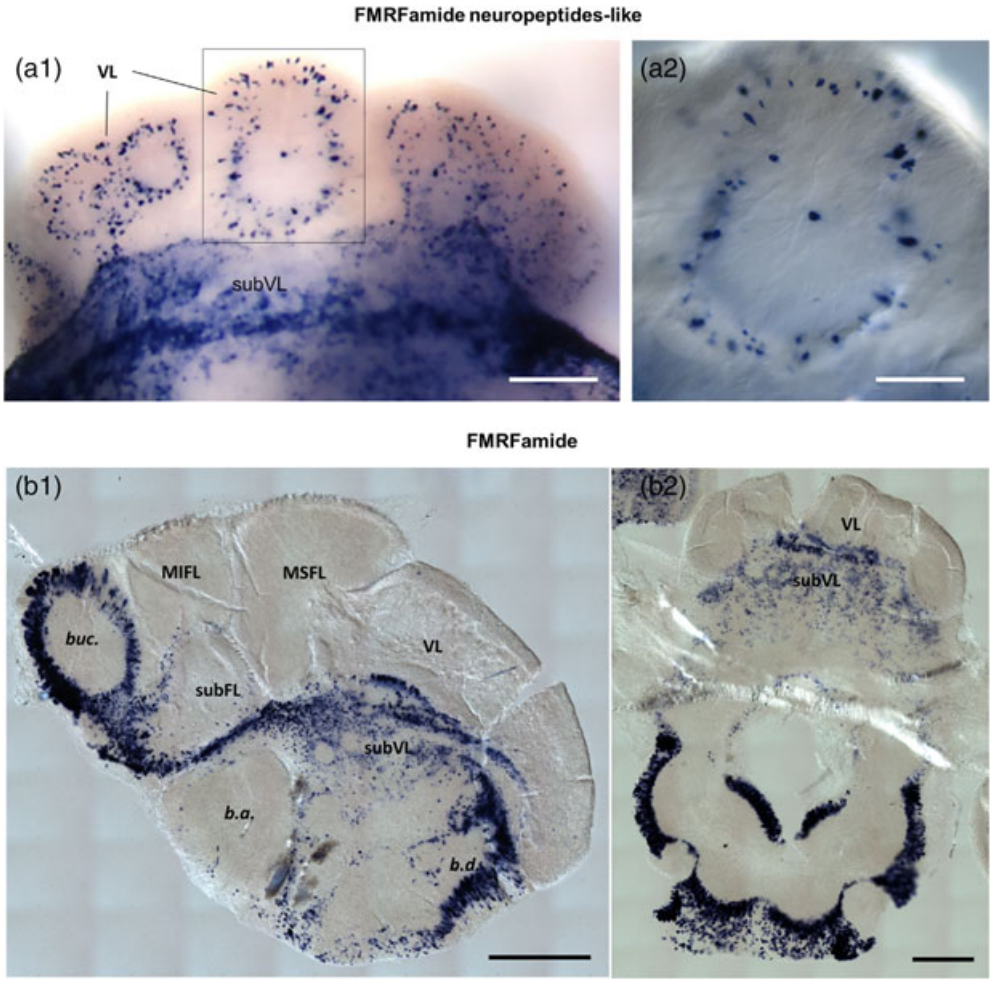

FIGURE 21 *Octopus vulgaris*, in situ staining of neuropeptide mRNA-expressing neurons in the VL system and other supraesophageal regions—FMRFamide-like neuropeptides. (a1) Transverse section showing FMRFamide-like peptide (FLRIamide) mRNA-expression in large cell bodies resembling LNs. The subVL also shows strong transcript expression. (a2) Enlargement of the area marked in A1 showing FLRIamide-expressing LNs in the medial lobule. (b1) Sagittal section showing FMRFamide mRNA-expressing cells in the supraesophageal brain. In addition to the abundant expression throughout the subVL, dorsal basal lobe (b.d) and buccal lobe (buc), some cells were detected in the ventral cell body cortex of the VL and subFL. (b2) Transverse slice showing FMRFamide mRNA-expressing cells in the subVL and subesophageal brain areas. Sparse labeling is also seen in the ventral cell cortex of the VL lobuli. Scale bars: 500 μm (a1, b2); 1 mm (b1), 200 μm (a2)

transmitter or co-transmitter. Members of a class of neuropeptides ending in RFamide are known to be depressive/inhibitory neuromodulators in mollusks (Zhang et al., 2012; Baux et al., 1990; Cottrell, 1993; van Golen et al., 1995), activating PKC and regulating cholinergic synapses (Baux et al., 1990), and they appear similar in other cephalopods (Chrachri & Williamson, 2003). Thus, this neuromodulator may be involved in long-term modulation—likely protein synthesis-dependent—in regions outside the VL, where long-term memories are stored. Similarly, FMRFamide has long-term inhibitory effects on the *Aplysia* sensory-motor synapse, a classical model for synaptic processes involved in learning and memory (Montarolo et al., 1988). However, the specific roles of RFamide-related peptides still need to be investigated in detail.

4.4 | Neuromodulation systems in the VL: Localization of putative NOS activity

NADPH-diaphorase is a reliable reporter of NOS activity in mollusks (Moroz, 2000; Moroz et al., 2005; Moroz et al., 1999; Cruz et al., 1997; Floyd et al., 1998). The NADPH-diaphorase method produced intense labeling in the AM neurites and VL neuropil, indicating NOS activity in these structures (Figure 17). NO is a well-known anterograde neurotransmitter in sensory and motor circuits of mollusks (Bodnarova et al., 2005; Hatcher et al., 2006; Moroz, 2006; Moroz & Gillette, 1995; Moroz & Kohn, 2011; Moroz et al., 1993; Moroz et al., 2000). NO also mediates synaptic plasticity in mollusks, including its own release from interneurons (Antonov et al., 2007; Katzoff et al., 2002; Kemenes et al., 2002; Korshunova & Balaban, 2014) and is involved in the LTP in octopus VL (Turchetti-Maia et al., 2018). The localization of NOS found here fits with physiological results that suggested the retrograde mediation of LTP by NO increasing the probability of glutamate release from the presynaptic terminals of the MSFL neurons. These accords with the view of a retrograde message inducing presynaptic expression of plasticity, a commonly postulated scheme for NO-mediated plasticity, including associative (Hebbian) learning in mammals (Arancio et al., 1996; Garthwaite, 2008; Prast & Philippu, 2001; Turchetti-Maia et al., 2017). The similar pattern of expression of NOS and cChAT in the VL and subFL neuropils supports the presence of NOS in the cholinergic AMs. As the AMs are the postsynaptic targets of the MSFL synapses, this supports NO as a retrograde messenger in the presynaptic expression of LTP (Turchetti-Maia et al., 2018).

We could not demonstrate NOS activity in the neuropil of cuttlefish *Sepia officinalis* VL (not shown), suggesting that the molecular mechanism mediating LTP in cephalopods evolved independently in

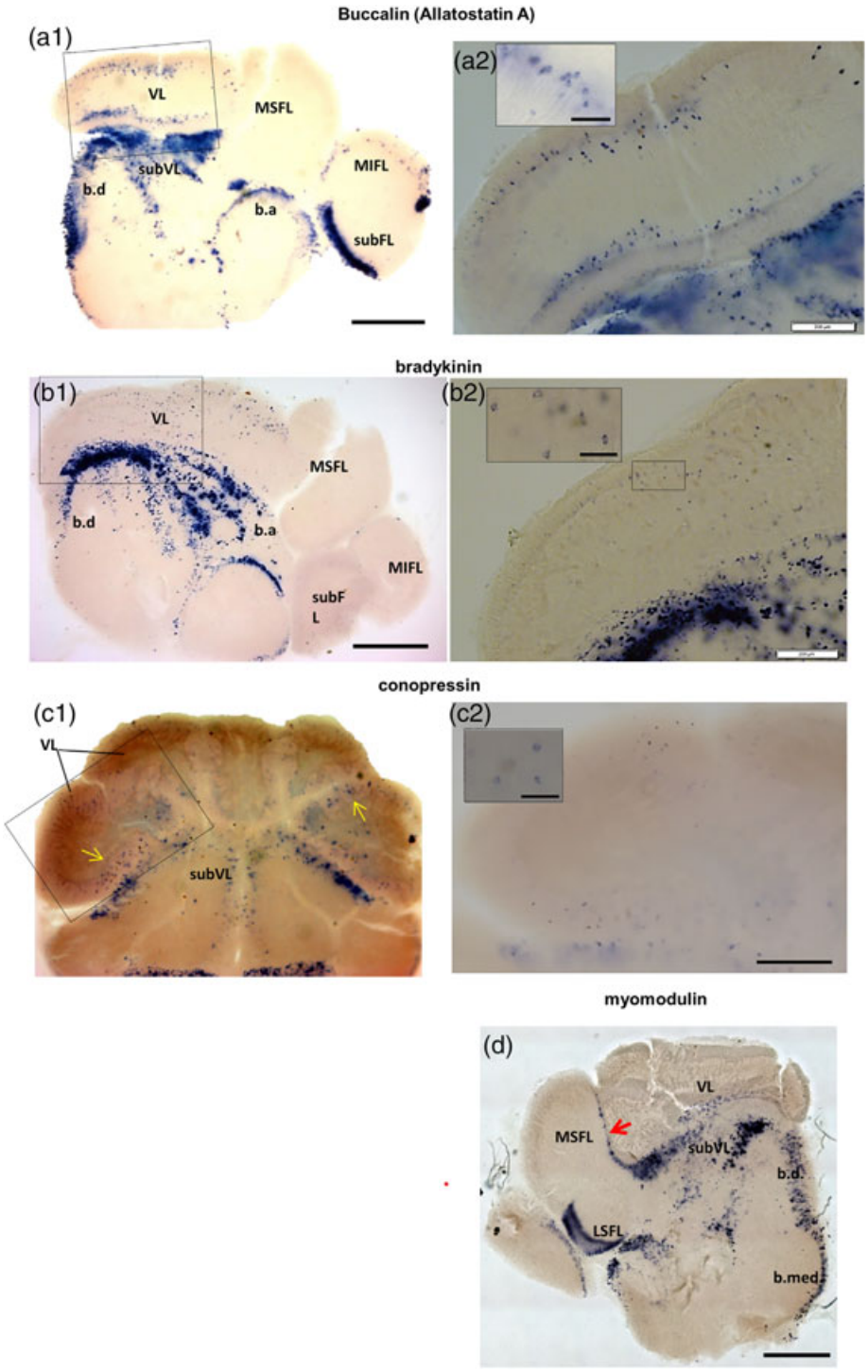

FIGURE 22 *Octopus vulgaris*, in situ staining of neuropeptide mRNA-expressing neurons in the VL system and other supraesophageal regions—Buccalin, bradykinin, conopressin, myomodulin. (a1) Sagittal section showing buccalin mRNA-expressing neurons in the dorsal and ventral cell layers in the VL in large cell bodies resembling LNs. There is also marked expression in the subVL, dorsal and anterior basal lobes and subFL cortices. (a2) Enlargement of the area marked in a1. Buccalin mRNA expressing individual cells are enlarged in the inset image. (b1) Sagittal section showing bradykinin mRNA-expressing cell bodies in the VL. Expression is especially strong in the subVL. (b2) Enlargement of the area marked in b1. Individual cells expressing bradykinin mRNA are enlarged in inset image. (c1) Transverse section showing conopressin mRNA-expressing neurons mainly, but not exclusively, in the lateral lobuli of the VL (arrows). (c2) Enlargement of the area marked in c1. Individual bradykinin-expressing cells are enlarged in inset image. Intense expression was observed in cells throughout the subVL. (d) Myomodulin transcript-expressing neurons are present in the border between the MSFL and the VL (arrow), in the subVL, basal lobes and lateral SFL (lSFL). There were no clear indications for expression within the VL itself. Scale bars: 500 μm (a1, b2); 1 mm (a1, b1, c1, d); 200 μm (a2, b2, d2); 50 μm (insets)

these phylogenetically close species as did the site of LTP (Shomrat et al., 2011).

4.5 | Tyrosine hydroxylase marker suggests catecholaminergic reward signaling in the VL system

Serotonin and octopamine have short-term facilitatory effects in the VL, reinforcing and suppressing LTP induction, respectively (Shomrat et al., 2010; Turchetti-Maia et al., 2017). TH, the enzyme which catalyzes the conversion of tyrosine into L-DOPA, the precursor of dopamine, was widely distributed in the MSFL and VL neuropil, indicating the involvement of catecholamines, particularly dopamine, in the MSF-VL neural network (Figures 18–20). These results confirm those of (Tansey, 1980), who reported scattered dopamine and/or other catecholamines in the MSFL and certain lobules in the VL neuropil, but not in the cell body layers. Here, a meshwork of thin TH-IR processes was seen in the outer neuropil in the region of the MSFL-AM synaptic connections (Figure 20). This agrees with findings that dopamine could mediate a short-term facilitatory effect on the

synaptic input to the AMs, while blocking the development of activity-dependent LTP (Weber, 2018).

TH staining was distributed in a stereotypical pattern in the inner VL neuropil, suggesting a specific interaction with the proximal dendrites of the LNs (Figure 20b). There was a strong resemblance between the TH and the GABA labeling in the area into which the LN dendrites project in the inner VL neuropil (see Figure 12). Catecholaminergic modulation and GABAergic innervation may thus occur at the same location, such as particular regions of the LN dendrites. Co-transmission, similar innervation, and synaptic locations of GABA and a catecholamine (probably dopamine) have been found in learning systems in mollusks (Díaz-Ríos et al., 2002) and mammals (Maher & Westbrook, 2008).

The TH staining contrasts with the NADPH-d labeling and cChAT-IR, which showed homogenous widespread distributions throughout the entire inner VL neuropil. A finer spreading of TH-labeled process into the cell cortex in the region of the synaptic connection between the MSFL terminals and the AMs (Figures 19b' and 20a) accords with the physiological finding of dopamine-dependent modulation of short- and long-term synaptic plasticity of these synaptic connections (Weber, 2018).

The abundantly labeled TH-IR cell bodies in the "deep nucleus" at the MSFL-VL border (Figure 18), may give rise to the TH-positive fibers running antero-posteriorly in the inner VL neuropil. This would imply that 5-HT inputs convey modulatory signals from other brain structures into the VL (Shomrat et al., 2010), like the global dopamine, noradrenaline, and acetylcholine fibers innervating the hippocampus (Matsuda et al., 2006) and modulatory inputs to the insect mushroom bodies (Fiala, 2007). But, in contrast, in the octopus VL, at least part of the TH modulation uniquely originates from within the MSFL-VL system itself, suggesting involvement in the control of the VL internal state.

Intense TH-IR neuronal processes crossing through the VL lobule hila (Figure 20b) showed broad interactions between the VL and surrounding lobes that may be related to the consolidation of long-term memory reinforced through LTP induction in the VL (Shomrat et al., 2010; Turchetti-Maia et al., 2017).

4.6 | Neuropeptides in the learning system

Several neuropeptide mRNAs were revealed in the MSFL, and VL (Figures 21, 22); buccalin, bradykinin, conopressin, and myomodulin showed expression mainly in the cell bodies within different areas. Such differential expression of neuropeptides may play an important role in setting the specific neurophysiological properties of the lobes and beyond. The functional roles of these and other neuropeptides deserve careful attention and separate exploration.

4.7 | Striking similarities between visual and tactile learning structures

The MSFL-VL, the visual learning system, and the MIFL-subFL, the tactile learning system, both show a fan-out fan-in network organization (Sanders, 1975; Young, 1971). The distribution of neuropeptides and NADPH-d staining in the MSFL-VL system (Figure 17) was strikingly similar to that in the MIFL-subFL system. Similar cChAT labeling (Figure 9) and GABA IHC patterns (Figure 15) were also found in the two lobes. The similar structure of the MIFL-subFL assisted us in interpreting the labeling in the VL, especially because the small cell bodies of the VL AMs, almost devoid of cytoplasm, seem not to express detectable amounts of synaptic proteins. Thus, the NADPH-d reactivity of the small cell bodies in the cell layer of the subFL supported the analysis of which interneurons in the VL probably also contained NOS activity (see Figure 14a); this approach gave a fit with our interpretations of AM neurite labeling in the VL. Analyzing the separate visual and tactile learning systems, with their similar organization, in terms of cell types, neurotransmitters, neuromodulators and physiology, could provide a better understanding of the overall functional organization of biological learning and memory systems controlling specific behaviors.

5 | CONCLUSION

Our results confirm previous anatomical and physiological findings of a feedforward fan-out fan-in network in the VL (Shomrat et al., 2011). The input *en passant* MSF-to-AM synapses are glutamatergic synapses that undergo LTP. A large group of AMs are cholinergic and mediate the fan-in excitatory input to the LNs.

Yet, immunohistochemical labeling revealed that the VL feedforward connectivity is not exclusively simpler and excitatory. Our findings suggest that MSFL glutamatergic inputs also innervate a GABAergic group of AMs, which likely feed modulatory or inhibitory inputs to the LNs. As mentioned above, an ongoing connectome study has revealed that a small proportion of the AMs have a complex bifurcating neurite tree. These "complex" AM, interneurons integrate synaptic inputs from the MSFL and "simple" AMs. This connectivity scheme makes these AMs plausible candidates for the inhibitory AMs. Furthermore, in contrast to previous assumptions, not all LNs are inhibitory; some neurons with large cell bodies were positively labeled for glutamate (and possibly ACh). Thus, the VL control of behavior seems to be intricately orchestrated by both excitatory and inhibitory pathways, providing more elaborated association modes for memory acquisition. Further physiological, anatomical and behavioral studies are needed to fully understand these pathways.

This study also contributes important insights into neuromodulatory systems, showing distributed innervation of TH-positive process in the VL, which suggest an elaborated catecholinergic neuromodulatory system. Physiological experiments have revealed the importance of serotonergic, dopaminergic, and octopaminergic modulatory reward and punishment signals in enhancing or suppressing LTP (reviewed in Turchetti-Maia et al., 2017).

Finally, in view of the proposed involvement of NO in the octopus LTP, the finding of robust expression of NADPH-d/NOS activity in the VL neuropil supports NO as a retrograde signal from the

postsynaptic AMs to the presynaptic MSFL terminal leading to an increase in presynaptic glutamate release (Turchetti-Maia et al., 2018).

ACKNOWLEDGMENTS

The authors wish to thank Dr. Tal Shomrat and Dr. Nir Nesher from the Ruppin Academic Center Israel for their technical and scientific help. The authors wish to thank Prof. H. Kimura and Dr. Jean-Pierre Bellier for providing cChAT antibody and for their helpful comments and suggestions. Special appreciation to Dr. Yael Friedman, Dr. Naomi Melamed-Book and Naomi Feinstein from the Bio-Imaging Unit, Hebrew University for their help with electron and confocal microscopy and to Prof. Jenny Kien for editing the manuscript. This work was supported by the United States - Israel Binational Science Foundation (BSF) (2007-407; 2011-466). Israel Sciences Foundation (ISF) (1425-2011; 1928-2015). (to B.H.) And in part by the Human Frontiers Science Program (RGP0060/2017) and National Science Foundation (1146575, 1557923, 1548121, 1645219) grants to L.L.M. Research reported in this publication was also supported in part by the National Institute of Neurological Disorders and Stroke of the National Institutes of Health under Award Number R01NS114491 (to L.L.M). The content is solely the authors' responsibility and does not necessarily represent the official views of the National Institutes of Health.

CONFLICT OF INTEREST

The authors declare no conflict of interest.

AUTHOR CONTRIBUTIONS

Naama Stern-Mentch: Conceptualization (equal); data curation (lead); formal analysis (equal); investigation (lead); methodology (lead); writing – original draft (equal). **Gabriela Winters:** Conceptualization (equal); data curation (supporting); formal analysis (equal); investigation (equal); methodology (equal); writing – original draft (equal). **Michael Belenky:** Data curation (supporting); formal analysis (supporting); methodology (equal); supervision (supporting). **Leonid Moroz:** Conceptualization (equal); funding acquisition (lead); methodology (equal); supervision (lead); writing – original draft (equal); writing – review and editing (equal). **Binyamin Hochner:** Conceptualization (equal); funding acquisition (lead); investigation (equal); methodology (equal); supervision (lead); writing – original draft (equal); writing – review and editing (equal).

PEER REVIEW

The peer review history for this article is available at https://publons.com/publon/10.1002/jmor.21459.

DATA AVAILABILITY STATEMENT

Data sharing is not applicable to this article as no new data were created or analyzed in this study.

ORCID

Leonid Moroz https://orcid.org/0000-0002-1333-3176
Binyamin Hochner https://orcid.org/0000-0002-9638-7320

REFERENCES

Albertin, C. B., Bonnaud, L., Brown, C. T., Crookes-Goodson, W. J., da Fonseca, R. R., Di Cristo, C., Dilkes, B. P., Edsinger-Gonzales, E., Freeman, R. M., Jr., Hanlon, R. T., Koenig, K. M., Lindgren, A. R., Martindale, M. Q., Minx, P., Moroz, L. L., Nodl, M. T., Nyholm, S. V., Ogura, A., Pungor, J. R., … Ragsdale, C. W. (2012). Cephalopod genomics: A plan of strategies and organization. *Standards in Genomic Sciences*, *7*(1), 175–188. https://doi.org/10.4056/sigs.3136559

Albertin, C. B., & Simakov, O. (2020). Cephalopod biology: At the intersection between genomic and organismal novelties. *Annual Review of Animal Biosciences*, *8*, 71–90.

Albertin, C. B., Simakov, O., Mitros, T., Wang, Z. Y., Pungor, J. R., Edsinger-Gonzales, E., Brenner, S., Ragsdale, C. W., & Rokhsar, D. S. (2015). The octopus genome and the evolution of cephalopod neural and morphological novelties. *Nature*, *524*(7564), 220–224.

Alves, C., Boal, J. G., & Dickel, L. (2008). Short-distance navigation in cephalopods: a review and synthesis. *Cognitive Processing*, *9*(4), 239–247.

Amodio, P., & Fiorito, G. (2013). Chapter 23 - Observational and Other Types of Learning in Octopus. In R. Menzel, & P. R. Benjamin (Eds.), *Handbook of Behavioral Neuroscience*, Vol. 22, pp. 293–302. Elsevier. https://doi.org/10.1016/B978-0-12-415823-8.00023-X

Antonov, I., Ha, T., Antonova, I., Moroz, L. L., & Hawkins, R. D. (2007). Role of nitric oxide in classical conditioning of siphon withdrawal in Aplysia. *The Journal of Neuroscience*, *27*(41), 10993–11002. https://doi.org/10.1523/jneurosci.2357-07.2007

Arancio, O., Kiebler, M., Lee, C. J., Lev-Ram, V., Tsien, R. Y., Kandel, E. R., & Hawkins, R. D. (1996). Nitric oxide acts directly in the presynaptic neuron to produce long-term Potentiationin in cultured hippocampal neurons. *Cell*, *87*(6), 1025–1035. https://doi.org/10.1016/S0092-8674(00)81797-3

Baux, G., Fossier, P., & Tauc, L. (1990). Histamine and FLRFamide regulate acetylcholine release at an identified synapse in Aplysia in opposite ways. *The Journal of Physiology*, *429*(1), 147–168.

Bidel, F., Meirovitch, Y., Schalek, L., Xiaotang, L., Yang, A., Berger, D., Peleg, A., Shaked, A., Flash, T., Lichtman, J., & Hochner, B. (2021). Insight into the connectome of the learning and memory network of the Octopus. Program No. P856.06. 2021 Neuroscience Meeting Planner. Society for Neuroscience

Boal, J. G. (1996). A review of simultaneous visual discrimination as a method of training octopuses. *BiolRev*, *71*, 157–190.

Bodnarova, M., Martasek, P., & Moroz, L. L. (2005). Calcium/calmodulin-dependent nitric oxide synthase activity in the CNS of Aplysia californica: Biochemical characterization and link to cGMP pathways. *Journal of Inorganic Biochemistry*, *99*(4), 922–928. https://doi.org/10.1016/j.jinorgbio.2005.01.012

Boycott, B. B. (1954). Learning in *Octopus vulgaris* and other cephalopods. *Pubbl Staz Zool, Napoli*, *25*, 67–93.

Boycott, B. B. (1961). The functional organization of the brain of the cuttlefishSepia officinalis. *Proceedings of the Royal Society of London B Biological Sciences*, *153*, 503–534.

Boycott, B. B., & Young, J. Z. (1955). A memory system in *Octopus vulgaris* Lamarck. *Proceedings of the Royal Society of London - Series B: Biological Sciences*, *143*(913), 449–480.

Boycott, B. B., & Young, J. Z. (1958). Reversal of learned responses in *Octopus vulgaris* Lamarck. *Animal Behaviour*, *6*, 45–52.

Brusca, R. C., & Brusca, G. J. (1990). *Invertebrates* (1st ed.). Sinauer Associates.

Bullock, T. H., & Horridge, G. A. (1965). *Structure and function in the nervous systems of invertebrates*. W. H. Freeman.

Casini, A., Vaccaro, R., D'Este, L., Sakaue, Y., Bellier, J. P., Kimura, H., & Renda, T. G. (2012). Immunolocalization of choline acetyltransferase of common type in the central brain mass of *Octopus vulgaris*. *European Journal of Histochemistry*, *56*(3), 215–222. https://doi.org/10.4081/ejh.2012.e34

Chrachri, A., & Williamson, R. (2003). Modulation of spontaneous and evoked EPSCs and IPSCs in optic lobe neurons of cuttlefish Sepia officinalis by the neuropeptide FMRF-amide. *European Journal of Neuroscience*, *17*(3), 526–536.

Cornwell, C. J., Messenger, J. B., & Williamson, R. (1993). Distribution of GABA-like immunoreactivity in the octopus brain. *Brain Research*, *621*(2), 353–357.

Cottrell, G. A. (1993). The wide range of actions of the FMRFamide-related peptides and the biological importance of peptidergic messengers. In Y. Pichon (Eds.), *Comparative Molecular Neurobiology*, Vol. 63. Birkhäuser Basel. https://doi.org/10.1007/978-3-0348-7265-2_15

Cruz, L., Moroz, L. L., Gillette, R., & Sweedler, J. V. (1997). Nitrite and nitrate levels in individual molluscan neurons: Single-cell capillary electrophoresis analysis. *Journal of Neurochemistry*, *69*(1), 110–115. https://doi.org/10.1046/j.1471-4159.1997.69010110.x

D'Este, L., Kimura, S., Casini, A., Matsuo, A., Bellier, J. P., Kimura, H., & Renda, T. G. (2008). First visualization of cholinergic cells and fibers by immunohistochemistry for choline acetyltransferase of the common type in the optic lobe and peduncle complex of *Octopus vulgaris*. *Journal of Comparative Neurology*, *509*(6), 566–579.

Di Cosmo, A., Di Cristo, C., & Messenger, J. B. (2006). L-glutamate and its ionotropic receptors in the nervous system of cephalopods. *Current Neuropharmacology*, *4*(4), 305–312. https://doi.org/10.2174/157015906778520809

Di Cosmo, A., Nardi, G., Di Cristo, C., De Santis, A., & Messenger, J. B. (1999). Localization of L-glutamate and glutamate-like recaptors at the squid giant synapse. *Brain Research*, *839*, 213–220.

Di Cosmo, A., Paolucci, M., & Di Cristo, C. (2004). N-methyl-D-aspartate receptor-like immunoreactivity in the brain of sepia and octopus. *The Journal of Comparative Neurology*, *477*(2), 202–219.

Di Cosmo, A., Pinelli, C., Scandurra, A., Aria, M., & D'Aniello, B. (2021). Research trends in octopus biological studies. *Animals (Basel)*, *11*, 1808. https://doi.org/10.3390/ani1106180

Díaz-Ríos, M., Oyola, E., & Miller, M. W. (2002). Colocalization of γ-aminobutyric acid-like immunoreactivity and catecholamines in the feeding network of Aplysia californica. *Journal of Comparative Neurology*, *445*(1), 29–46.

Erwin, D. H., & Valentine, J. W. (2013). *The Cambrian explosion: The reconstruction of animal biodiversity* (p. 406). Roberts and Co.

Fiala, A. (2007). Olfaction and olfactory learning in drosophila: Recent progress. *Current Opinion in Neurobiology*, *17*(6), 720–726.

Fiorito, G., Affuso, A., Anderson, D. B., Basil, J., Bonnaud, L., Botta, G., Cole, A., D'Angelo, L., De Girolamo, P., & Dennison, N. (2014). Cephalopods in neuroscience: Regulations, research and the 3Rs. *Invertebrate Neuroscience*, *14*(1), 13–36.

Fiorito, G., Affuso, A., Basil, J., Cole, A., de Girolamo, P., D'angelo, L., Dickel, L., Gestal, C., Grasso, F., & Kuba, M. (2015). Guidelines for the care and welfare of cephalopods in research—A consensus based on an initiative by CephRes, FELASA and the Boyd Group. *Laboratory Animals*, *49*, 1–90.

Fiorito, G., & Chichery, R. (1995). Lesions of the vertical lobe impair visual-discrimination learning by observation in octopus-vulgaris. *Neuroscience Letters*, *192*(2), 117–120.

Fiorito, G., & Scotto, P. (1992). Observational-learning in octopus-vulgaris. *Science*, *256*(5056), 545–547.

Fiorito, G., von Planta, C., & Scotto, P. (1990). Problem solving ability of *Octopus vulgaris* Lamarck (Mollusca, Cephalopoda). *Behavioral and Neural Biology*, *53*(2), 217–230.

Floyd, P. D., Moroz, L. L., Gillette, R., & Sweedler, J. V. (1998). Capillary electrophoresis analysis of nitric oxide synthase related metabolites in single identified neurons. *Analytical Chemistry*, *70*(11), 2243–2247. https://doi.org/10.1021/ac9713013

Fuchs, D., Hoffmann, R., & Klug, C. (2021). Evolutionary development of the cephalopod arm armature: A review. *Swiss Journal of Palaeontology*, *140*(1), 27.

Garthwaite, J. (2008). Concepts of neural nitric oxide-mediated transmission. *European Journal of Neuroscience*, *27*(11), 2783–2802. https://doi.org/10.1111/j.1460-9568.2008.06285.x

Graindorge, N., Alves, C., Darmaillacq, A. S., Chichery, R., Dickel, L., & Bellanger, C. (2006). Effects of dorsal and ventral vertical lobe electrolytic lesions on spatial learning and locomotor activity in Sepia officinalis. *Behavioral Neuroscience*, *120*(5), 1151–1158.

Graindorge, N., Jozet-Alves, C., Chichery, R., Dickel, L., & Bellanger, C. (2008). Does kainic acid induce partial brain lesion in an invertebrate model: Sepia officinalis? Comparison with electrolytic lesion. *Brain Research*, *1238*, 44–52.

Gray, E. G. (1970). The fine structure of the vertical lobe of octopus brain. *Philosophical Transactions of the Royal Society B*, *258*, 379–394.

Gutnick, T., Byrne, R. A., Hochner, B., & Kuba, M. (2011). *Octopus vulgaris* uses visual information to determine the location of its arm. *Current Biology*, *21*(6), 460–462.

Gutnick, T., Zullo, L., Hochner, B., & Kuba, M. J. (2020). Use of peripheral sensory information for central nervous control of arm movement by *Octopus vulgaris*. *Current Biology*, *30*(21), 4322–4327.e4323. https://doi.org/10.1016/j.cub.2020.08.037

Hanlon, R. T., & Messenger, J. B. (2018). *Cephalopod behaviour*. Cambridge University Press.

Hatcher, N. G., Sudlow, L. C., Moroz, L. L., & Gillette, R. (2006). Nitric oxide potentiates cAMP-gated cation current in feeding neurons of Pleurobranchaea californica independent of cAMP and cGMP signaling pathways. *Journal of Neurophysiology*, *95*(5), 3219–3227. https://doi.org/10.1152/jn.00815.2005

Heisenberg, M. (2003). Mushroom body memoir: From maps to models. *Nature Reviews. Neuroscience*, *4*(4), 266–275.

Hildenbrand, A., Austermann, G., Fuchs, D., Bengtson, P., & Stinnesbeck, W. (2021). A potential cephalopod from the early Cambrian of eastern Newfoundland, Canada. *Communications Biology*, *4*(1), 388.

Hochner, B., Brown, E. R., Langella, M., Shomrat, T., & Fiorito, G. (2003). A learning and memory area in the octopus brain manifests a vertebrate-like long-term potentiation. *Journal of Neurophysiology*, *90*(5), 3547–3554.

Hochner, B., Shomrat, T., & Fiorito, G. (2006). The octopus: A model for a comparative analysis of the evolution of learning and memory mechanisms. *The Biological Bulletin*, *210*, 308–317. https://doi.org/10.2307/4134567

Hochner, B., & Glanzman, D. L. (2016). Evolution of highly diverse forms of behavior in molluscs. *Current Biology*, *26*(20), R965–R971.

Hoffmann, R., Bestwick, J., Berndt, G., Berndt, R., Fuchs, D., & Klug, C. (2020). Pterosaurs ate soft-bodied cephalopods (Coleoidea). *Scientific Reports*, *10*(1), 1230.

Hope, B., & Vincent, S. (1989). Histochemical characterization of neuronal NADPH-diaphorase. *Journal of Histochemistry & Cytochemistry*, *37*(5), 653–661.

Jezzini, S. H., Bodnarova, M., & Moroz, L. L. (2005). Two-color in situ hybridization in the CNS of Aplysia californica. *Journal of Neuroscience Methods*, *149*(1), 15–25. https://doi.org/10.1016/j.jneumeth.2005.05.007

Kandel, E., Schwartz, J., Jessell, T., Siegelbaum, S., & Hudspeth, A. J. (2012). *Principles of neural science* (5th ed.). McGraw-Hill Education.

Katzoff, A., Ben-Gedalya, T., & Susswein, A. J. (2002). Nitric oxide is necessary for multiple memory processes after learning that a food is inedible in Aplysia. *The Journal of Neuroscience*, *22*(21), 9581–9594.

Kemenes, I., Kemenes, G., Andrew, R. J., Benjamin, P. R., & O'Shea, M. (2002). Critical time-window for NO–cGMP-dependent long-term memory formation after one-trial appetitive conditioning. *The Journal of Neuroscience*, *22*(4), 1414–1425.

Korshunova, T., & Balaban, P. (2014). Nitric oxide is necessary for long-term facilitation of synaptic responses and for development of context memory in terrestrial snails. *Neuroscience*, *266*, 127–135.

Liscovitch-Brauer, N., Alon, S., Porath, H. T., Elstein, B., Unger, R., Ziv, T., Admon, A., Levanon, E. Y., Rosenthal, J. J., & Eisenberg, E. (2017). Trade-off between transcriptome plasticity and genome evolution in cephalopods. *Cell*, *169*, 191–202.e11.

Livneh, Y., Feinstein, N., Klein, M., & Mizrahi, A. (2009). Sensory input enhances synaptogenesis of adult-born neurons. *Journal of Neuroscience*, *29*(1), 86–97.

Mackintosh, N. J. (1965). Discrimination learning in the octopus. *Animal Behaviour*, *1*, 129–134.

Maher, B. J., & Westbrook, G. L. (2008). Co-transmission of dopamine and GABA in periglomerular cells. *Journal of Neurophysiology*, *99*(3), 1559–1564.

Maldonado, H. (1963). The visual attack learning system in *Octopus vulgaris*. *Journal of Theoretical Biology*, *5*(3), 470–488.

Maldonado, H. (1965). The positive and negative learning process in *Octopus vulgaris* Lamarck. Influence of the vertical and median superior frontal lobes. *Zeitschrift fur vergleichende Physiologie*, *51*, 185–203.

Mallatt, J., & Feinberg, T. E. (2021). Multiple routes to animal consciousness: Constrained multiple realizability rather than modest identity theory. *Frontiers in Psychology*, *12*, 732336.

Matsuda, Y., Marzo, A., & Otani, S. (2006). The presence of background dopamine signal converts long-term synaptic depression to potentiation in rat prefrontal cortex. *Journal of Neuroscience*, *26*(18), 4803–4810.

Messenger, J. B. (1996). Neurotransmitters of cephalopods. *Invertebrate Neuroscience*, *2*, 95–114.

Montarolo, P. G., Kandel, E. R., & Schacher, S. (1988). Long-term heterosynaptic inhibition in Aplysia. *Nature*, *333*(6169), 171–174.

Moriyama, T., & Gunji, Y. P. (1997). Autonomous learning in maze solution by Octopus. *Ethology*, *103*(6), 499–513.

Moroz, L. L. (2000). Giant identified NO-releasing neurons and comparative histochemistry of putative nitrergic systems in gastropod molluscs. *Microscopy Research and Technique*, *49*(6), 557–569. https://doi.org/10.1002/1097-0029(20000615)49:6<557::AID-JEMT6>3.0.CO;2-S

Moroz, L. L. (2006). Localization of putative nitrergic neurons in peripheral chemosensory areas and the central nervous system of Aplysia californica. *The Journal of Comparative Neurology*, *495*(1), 10–20. https://doi.org/10.1002/cne.20842

Moroz, L. L. (2009). On the independent origins of complex brains and neurons. *Brain, Behavior and Evolution*, *74*(3), 177–190.

Moroz, L. L., Dahlgren, R. L., Boudko, D., Sweedler, J. V., & Lovell, P. (2005). Direct single cell determination of nitric oxide synthase related metabolites in identified nitrergic neurons. *Journal of Inorganic Biochemistry*, *99*(4), 929–939. https://doi.org/10.1016/j.jinorgbio.2005.01.013

Moroz, L. L., & Gillette, R. (1995). From Polyplacophora to Cephalopoda: Comparative analysis of nitric oxide signalling in mollusca. *Acta Biologica Hungarica*, *46*(2–4), 169–182.

Moroz, L. L., Gillette, R., & Sweedler, J. V. (1999). Single-cell analyses of nitrergic neurons in simple nervous systems. *The Journal of Experimental Biology*, *202*(Pt 4), 333–341.

Moroz, L. L., Gyori, J., & Salanki, J. (1993). NMDA-like receptors in the CNS of molluscs. *Neuroreport*, *4*(2), 201–204. https://doi.org/10.1097/00001756-199302000-00022

Moroz, L. L., & Kohn, A. B. (2010). Do different neurons age differently? Direct genome-wide analysis of aging in single identified cholinergic neurons. *Frontiers in Aging Neuroscience*, *2*, 6. https://doi.org/10.3389/neuro.24.006.2010

Moroz, L. L., & Kohn, A. B. (2011). Parallel evolution of nitric oxide signaling: Diversity of synthesis and memory pathways. *Frontires Bioscience*, *16*, 2008–2051. https://doi.org/10.2741/3837Moroz

Moroz, L. L., Nikitin, M. A., Poličar, P. G., Kohn, A. B., & Romanova, D. Y. (2021). Evolution of glutamatergic signaling and synapses. *Neuropharmacology*, in press.

Moroz, L. L., Norekian, T. P., Pirtle, T. J., Robertson, K. J., & Satterlie, R. A. (2000). Distribution of NADPH-diaphorase reactivity and effects of nitric oxide on feeding and locomotory circuitry in the pteropod mollusc Clione limacina. *Journal of Comparative Neurology*, *427*(2), 274–284.

Moroz, L. L., Park, J. H., & Winlow, W. (1993). Nitric oxide activates buccal motor patterns in Lymnaea stagnalis. *Neuroreport*, *4*(6), 643–646. https://doi.org/10.1097/00001756-199306000-00010

Neal, S., McCulloch, K. J., Napoli, F. R., Daly, C. M., Coleman, J. H., & Koenig, K. M. (2022). Co-option of the limb patterning program in cephalopod eye development. *BMC Biology*, *20*(1), 1.

Nesher, N., Levy, G., Zullo, L., & Hochner, B. (2020). *Octopus motor control*. Oxford University Press. https://doi.org/10.1093/acrefore/9780190264086.013.283

Nieder, A. (2021). Neuroethology of number sense across the animal kingdom. *Journal of Experimental Biology*, *224*(6), jeb218289.

Nixon, M., & Young, J. Z. (2003). *The brains and lives of cephalopods*. Oxford University Press.

Papini, M. R., & Bitterman, M. E. (1991). Appetitive conditioning in Octopus cyanea. *Journal of Comparative Psychology*, *105*(2), 107–114.

Packard, A. (1972). Cephalopods and fish: the limits of convergence. *Biological Reviews*, 47, 241–307.

Prast, H., & Philippu, A. (2001). Nitric oxide as modulator of neuronal function. *Progress in Neurobiology*, *64*(1), 51–68. https://doi.org/10.1016/S0301-0082(00)00044-7

Puthanveettil, S. V., Antonov, I., Kalachikov, S., Rajasethupathy, P., Choi, Y. B., Kohn, A. B., Citarella, M., Yu, F., Karl, K. A., Kinet, M., Morozova, I., Russo, J. J., Ju, J., Moroz, L. L., & Kandel, E. R. (2013). A strategy to capture and characterize the synaptic transcriptome. *Proceedings of the National Academy of Sciences of the United States of America*, *110*(18), 7464–7469. https://doi.org/10.1073/pnas.1304422110

Richter, J. N., Hochner, B., & Kuba, M. J. (2015). Octopus arm movements under constrained conditions: Adaptation, modification and plasticity of motor primitives. *The Journal of Experimental Biology*, *218*(7), 1069–1076. https://doi.org/10.1242/jeb.115915

Richter, J. N., Hochner, B., & Kuba, M. J. (2016). Pull or push? Octopuses solve a puzzle problem. *PLoS One*, *11*(3), e0152048.

Rosenblatt, F. (1958). The perceptron: A probabilistic model for information storage and organization in the brain. *Psychological Review*, *65*(6), 386–408. https://doi.org/10.1037/h0042519

Sakaue, Y., Bellier, J.-P., Kimura, S., D'Este, L., Takeuchi, Y., & Kimura, H. (2014). Immunohistochemical localization of two types of choline acetyltransferase in neurons and sensory cells of the octopus arm. *Brain Structure & Function*, *219*(1), 323–341. https://doi.org/10.1007/s00429-012-0502-6

Sanders, G. D. (1975). The cephalopods. In W. C. Corning, J. A. Dyal, & A. O. D. Willows (Eds.), *Invertebrate learning* (Vol. 3, pp. 139–145). Plenum Press.

Schnell, A. K., Amodio, P., Boeckle, M., & Clayton, N. S. (2021). How intelligent is a cephalopod? Lessons from comparative cognition. *Biological Reviews of the Cambridge Philosophical Society*, *96*(1), 162–178.

Shigeno, S., & Ragsdale, C. W. (2015). The gyri of the octopus vertical lobe have distinct neurochemical identities. *The Journal of Comparative Neurology*, *523*(9), 1297–1317. https://doi.org/10.1002/cne.23755

Shomrat, T., Feinstein, N., Klein, M., & Hochner, B. (2010). Serotonin is a facilitatory neuromodulator of synaptic transmission and "reinforces" long-term potentiation induction in the vertical lobe of *Octopus vulgaris*. *Neuroscience*, *169*(1), 52–64.

Shomrat, T., Graindorge, N., Bellanger, C., Fiorito, G., Loewenstein, Y., & Hochner, B. (2011). Alternative sites of synaptic plasticity in two homologous fan-out fan-in learning and memory networks. *Current Biology*, *21*(21), 1773–1782.

Shomrat, T., Turchetti-Maia, A. L., Stern-Mentch, N., Basil, J. A., & Hochner, B. (2015). The vertical lobe of cephalopods: An attractive

brain structure for understanding the evolution of advanced learning and memory systems. *Journal of Comparative Physiology. A*, *201*(9), 947–956. https://doi.org/10.1007/s00359-015-1023-6

Shomrat, T., Zarrella, I., Fiorito, G., & Hochner, B. (2008). The octopus vertical lobe modulates short-term learning rate and uses LTP to acquire long-term memory. *Current Biology*, *18*(5), 337–342. https://doi.org/10.1016/j.cub.2008.01.056

Striedter, G. F., Belgard, T. G., Chen, C. C., Davis, F. P., Finlay, B. L., Gunturkun, O., Hale, M. E., Harris, J. A., Hecht, E. E., Hof, P. R., Hofmann, H. A., Holland, L. Z., Iwaniuk, A. N., Jarvis, E. D., Karten, H. J., Katz, P. S., Kristan, W. B., Macagno, E. R., Mitra, P. P., … Wilczynski, W. (2014). NSF workshop report: Discovering general principles of nervous system organization by comparing brain maps across species. *The Journal of Comparative Neurology*, *522*(7), 1445–1453. https://doi.org/10.1002/cne.23568

Sutherland, N. S. (1959). Visual discrimination of shape by octopus. Circles and squares, and circles and triangles. *The Quarterly Journal of Experimental Psychology*, *11*, 24–32.

Taghert, P. H., & Nitabach, M. N. (2012). Peptide neuromodulation in invertebrate model systems. *Neuron*, *76*(1), 82–97.

Tansey, E. M. (1979). Neurotransmitters in the cephalopod brain. *Comparative Biochemistry and Physiology*, *64C*, 173–182.

Tansey, E. M. (1980). Aminergic fluorescence in the cephalopod brain. *Philosophical Transactions Of The Royal Society Of London Series B-Biological Sciences*, *291*(1046), 127–145.

Turchetti-Maia, A., Shomrat, T., & Hochner, B. (2017). *The vertical lobe of cephalopods—A brain structure ideal for exploring the mechanisms of complex forms of learning and memory* (pp. 1–27). Oxford University Press.

Turchetti-Maia, A. L., Stern-Mentch, N., Bidel, F., Nesher, N., Shomrat, T., & Hochner, B. (2018). A novel NO-dependent 'molecular-memory-switch' mediates presynaptic expression and postsynaptic maintenance of LTP in the octopus brain. *bioRxiv:491340*. https://doi.org/10.1101/491340

van Golen, F. A., Li, K. W., de Lange, R. P., Jespersen, S., & Geraerts, W. P. (1995). Mutually exclusive neuronal expression of peptides encoded by the FMRFa gene underlies a differential control of copulation in Lymnaea. *Journal of Biological Chemistry*, *270*(47), 28487–28493.

Vapnik, V. N. (1998). *Statistical learning theory*. Wiley.

Vehovszky, Á., Szabó, H., & Elliott, C. J. (2004). Octopamine-containing (OC) interneurons enhance central pattern generator activity in sucrose-induced feeding in the snail Lymnaea. *Journal of Comparative Physiology. A*, *190*(10), 837–846.

Villar-Cerviño, V., Barreiro-Iglesias, A., Fernández-lópez, B., Mazan, S., Rodicio, M. C., & Anadón, R. (2013). Glutamatergic neuronal populations in the brainstem of the sea lamprey, Petromyzon marinus: An in situ hybridization and immunocytochemical study. *Journal of Comparative Neurology*, *521*(3), 522–557.

Weber, I. (2018). MSc Thesis, Faculty of Science, Hebrew University of Jerusalem.

Wells, M. J. (1978). *Octopus*. Chapman and Hall.

Wentzell, M. M., Martínez-Rubio, C., Miller, M. W., & Murphy, A. D. (2009). Comparative neurobiology of feeding in the Opisthobranch Sea Slug, Aplysia, and the Pulmonate Snail, Helisoma: Evolutionary considerations. *Brain, Behavior and Evolution*, *74*(3), 219–230. https://doi.org/10.1159/000258668

Winters, G. C. (2018). *Molecular mapping of the octopus brain* (PhD dissertation). University of Florida. https://ufdc.ufl.edu/UFE0054028/00001.

Winters, G. C., Polese, G., Di Cosmo, A., & Moroz, L. L. (2020). Mapping of neuropeptide Y expression in Octopus brains. *Journal of Morphology*, *281*(7), 790–801. https://doi.org/10.1002/jmor.21141

Wolff, G. H., & Strausfeld, N. J. (2016). Genealogical correspondence of a forebrain Centre implies an executive brain in the protostome–deuterostome bilaterian ancestor. *Philosophical Transactions of the Royal Society B*, *371*(1685), 20150055.

Yeckel, M. F., Kapur, A., & Johnston, D. (1999). Multiple forms of LTP in hippocampal CA3 neurons use a common postsynaptic mechanism. *Nature Neuroscience*, *2*(7), 625–633.

Yoshida, M. A., Ogura, A., Ikeo, K., Shigeno, S., Moritaki, T., Winters, G. C., Kohn, A. B., & Moroz, L. L. (2015). Molecular evidence for convergence and parallelism in evolution of complex brains of cephalopod Molluscs: Insights from visual systems. *Integrative and Comparative Biology*, *55*(6), 1070–1083. https://doi.org/10.1093/icb/icv049

Young, J. Z. (1971). *The anatomy of the nervous system of Octopus vulgaris*. Clarendon Press.

Young, J. Z. (1991). Computation in the learning-system of cephalopods. *Biological Bulletin*, *180*(2), 200–208.

Young, J. Z. (1995). Multiple matrices in the memory system of octopus. In J. N. Abbott, R. Williamson, & L. Maddock (Eds.), *Cephalopod neurobiology* (pp. 431–443). Oxford University Press.

Zhang, Z., Goodwin, E., Loi, P. K., & Tublitz, N. J. (2012). Molecular analysis of a novel FMRFamide-related peptide gene (SOFaRP2) and its expression pattern in the brain of the European cuttlefish Sepia officinalis. *Peptides*, *34*(1), 114–119. https://doi.org/10.1016/j.peptides.2011.07.011

SUPPORTING INFORMATION

Additional supporting information may be found in the online version of the article at the publisher's website.

How to cite this article: Stern-Mentch, N., Bostwick, G. W., Belenky, M., Moroz, L., & Hochner, B. (2022). Neurotransmission and neuromodulation systems in the learning and memory network of Octopus vulgaris. *Journal of Morphology*, *283*(5), 557–584. https://doi.org/10.1002/jmor.21459